Search for high-mass dilepton resonances in pp collisions at $\sqrt{s} = 8$ TeV with the ATLAS detector

G. Aad *et al.*[*]
(ATLAS Collaboration)

(Received 16 May 2014; published 19 September 2014)

The ATLAS detector at the Large Hadron Collider is used to search for high-mass resonances decaying to dielectron or dimuon final states. Results are presented from an analysis of proton-proton (pp) collisions at a center-of-mass energy of 8 TeV corresponding to an integrated luminosity of 20.3 fb^{-1} in the dimuon channel. A narrow resonance with Standard Model Z couplings to fermions is excluded at 95% confidence level for masses less than 2.79 TeV in the dielectron channel, 2.53 TeV in the dimuon channel, and 2.90 TeV in the two channels combined. Limits on other model interpretations are also presented, including a grand-unification model based on the E_6 gauge group, Z^* bosons, minimal Z' models, a spin-2 graviton excitation from Randall-Sundrum models, quantum black holes, and a minimal walking technicolor model with a composite Higgs boson.

DOI: 10.1103/PhysRevD.90.052005 PACS numbers: 12.60.Cn, 13.85.Qk, 14.80.Rt, 14.80.Tt

I. INTRODUCTION

The current energy frontier can be explored in the invariant mass spectrum of dielectron or dimuon pairs via a search for new massive resonances at the Large Hadron Collider (LHC). Such a search has been performed using the full 8 TeV center-of-mass energy proton-proton (pp) collision data set of about 20 fb^{-1} recorded with the ATLAS detector [1] in 2012.

While the Standard Model (SM) has been confirmed at the LHC, the identification of massive dilepton resonances in proton-proton collisions still constitutes one of the most promising channels in searches for new physics. It implies a fully reconstructed signal over a smooth and well-understood background. Models with dilepton resonances are predicted in many scenarios for new physics. Among these are grand-unification models, which are motivated by gauge unification or a restoration of the left-right symmetry violated by the weak interaction. These models predict the existence of additional neutral, spin-1 vector gauge bosons called Z' bosons, due to the existence of larger symmetry groups that break to yield the SM gauge group and additional $U(1)$ gauge groups. Examples considered in this article include the Z' bosons of the E_6-motivated [2,3] and minimal models [4]. Another Z' signal, the Z'_{SSM}, is considered due to its inherent simplicity and usefulness as a benchmark model. The sequential Standard Model (SSM) includes a Z'_{SSM} boson with couplings to fermions equivalent to those of the SM Z boson.

Dilepton resonances are also predicted by several models motivated by solutions to the hierarchy problem of the SM, which involves the need to reconcile the very different scales of electroweak symmetry breaking and the gravitational Planck scale (M_{Pl}). The search for physics beyond the SM remains as crucial as it was prior to the discovery of the Higgs boson at the LHC [5,6], since solving the hierarchy problem is one of the primary objectives of the LHC physics program. Examples of potential signals in models that address the hierarchy problem are the Z^* [7–10] boson, the spin-2 graviton excitation in Randall-Sundrum (RS) models [11], quantum black holes (QBHs) [12], and technimesons in minimal walking technicolor (MWT) [13–16]. These, along with the Z' interpretations motivated by grand unification, are further discussed in Sec. II.

To conduct the search, the dilepton invariant mass ($m_{\ell\ell}$) line shape is examined for a localized excess of events corresponding to a new resonance, where $\ell\ell$ corresponds to either the dielectron or dimuon final state. This is done using signal and background templates that provide the expected yield of events in bins of $m_{\ell\ell}$. The methodology is fully described in Sec. XI. This search approach is advantageous because using the full shape of the distribution makes the analysis robust against uncertainties in the background model at high mass. If shape information were not used in the analysis, uncertainty in the background estimate would be more likely to mask a potential signal. The shape-based method is also more sensitive to a signal in the case of a signal with a low-mass tail arising from off-shell production, which occurs due to the steeply falling parton distribution function (PDF) of the two colliding partons at large values of Bjorken x. This feature is commonly referred to as a "parton-luminosity tail," and its size increases with the resonance width. The impact of

*Full author list given at the end of the article.

this parton-luminosity tail on the $m_{\ell\ell}$ distribution grows as the kinematic limit is approached.

The models considered here predict resonances that are narrow relative to the detector resolution. In such cases, interference effects, where they occur, are not expected to significantly alter the line shape and are thus not considered. The exception to this is the class of minimal Z' models described in Sec. II, for which large coupling strengths, and hence larger widths, are considered. In this case, interference effects are included explicitly in the analysis.

The potential signals studied in this analysis vary in width and spin, and some exhibit a parton-luminosity tail while others do not. Because of this, the final results given in Sec. XII can be interpreted in the context of other models that are not directly studied here, but that predict resonances in the $m_{\ell\ell}$ spectrum with similar signal shapes.

II. DESCRIPTION AND STATUS OF THEORETICAL MODELS

A detailed description of the models studied in this article is given in this section. For most models, the best previous limits from the ATLAS experiment were obtained using 5 fb^{-1} of data at $\sqrt{s} = 7$ TeV [17], while the exclusion results from the CMS experiment are based on 5 fb^{-1} of data at $\sqrt{s} = 7$ TeV and 4 fb^{-1} of data at $\sqrt{s} = 8$ TeV [18]. The data collected at 7 TeV have not been used to obtain the results presented in this paper, as doing so would not significantly extend the sensitivity of the search. Previous limits on the mass scale for QBH production are obtained from other sources, as noted in Sec. II E.

For the benchmark model, previous results from ATLAS exclude a Z'_{SSM} boson with mass less than 2.22 TeV at 95% confidence level (C.L.), while previous results from the CMS experiment exclude a Z'_{SSM} boson with mass less than 2.59 TeV at 95% C.L. Direct searches at the Tevatron experiments [19,20] and indirect constraints from LEP [21–24] have resulted in limits on the Z'_{SSM} mass of 1.071 [20] and 1.787 TeV [25], respectively.

A. E_6-motivated Z' models

In the class of models based on the E_6 gauge group, this unified symmetry group can break to the SM in a number of different ways [2]. In many of them, E_6 is first broken to $SO(10) \times U(1)_\psi$, with $SO(10)$ then breaking either to $SU(4) \times SU(2)_{\mathrm{L}} \times SU(2)_{\mathrm{R}}$ or $SU(5) \times U(1)_\chi$. In the first of these two possibilities, a $Z'_{3\mathrm{R}}$ coming from $SU(2)_{\mathrm{R}}$ or a $Z'_{\mathrm{B\text{-}L}}$ from the breaking of $SU(4)$ into $SU(3)_{\mathrm{C}} \times U(1)_{\mathrm{B\text{-}L}}$ could exist at the TeV scale. Both of these Z' bosons appear in the minimal Z' models discussed in the next section.

In the $SU(5)$ case, the presence of $U(1)_\psi$ and $U(1)_\chi$ symmetries implies the existence of associated gauge bosons Z'_ψ and Z'_χ that can mix. When $SU(5)$ is broken down to the SM, one of the $U(1)$'s can remain unbroken down to intermediate energy scales [2,3]. Therefore, the precise model is governed by a mixing angle θ_{E_6}, with the new potentially observable Z' boson defined by $Z'(\theta_{E_6}) = Z'_\psi \cos\theta_{E_6} + Z'_\chi \sin\theta_{E_6}$. The value of θ_{E_6} specifies the Z' boson's coupling strength to SM fermions as well as its intrinsic width. In comparison to the benchmark Z'_{SSM}, which has a width of approximately 3% of its mass, the E_6 models predict narrower Z' signals. The Z'_ψ considered here has a width of 0.5% of its mass, and the Z'_χ has a width of 1.2% of its mass [26,27]. All other Z' signals in this model are defined by specific values of θ_{E_6} ranging from 0 to π, and have widths between those of the Z'_ψ and Z'_χ.

Previous results from ATLAS exclude the Z'_ψ (Z'_χ) boson with mass less than 1.79 TeV (1.97 TeV) at 95% C.L. [17], while the CMS experiment excludes a Z'_ψ boson with mass less than 2.26 TeV at 95% C.L. [18].

B. Minimal Z' models

In the minimal Z' models [4], the phenomenology of Z' boson production and decay is characterized by three parameters: two effective coupling constants, $g_{\mathrm{B\text{-}L}}$ and g_{Y}, and the Z' boson mass. This parametrization encompasses Z' bosons from many models, including the Z'_χ belonging to the E_6-motivated model of the previous section, the $Z'_{3\mathrm{R}}$ in a left-right symmetric model [28,29], and the $Z'_{\mathrm{B\text{-}L}}$ of the pure B-L model [30], where B (L) is the baryon (lepton) number and B-L is the conserved quantum number. The coupling parameter $g_{\mathrm{B\text{-}L}}$ defines the coupling of a new Z' boson to the B-L current, while the g_{Y} parameter represents the coupling to the weak hypercharge Y. It is convenient to refer to the ratios $\tilde{g}_{\mathrm{B\text{-}L}} \equiv g_{\mathrm{B\text{-}L}}/g_Z$ and $\tilde{g}_{\mathrm{Y}} \equiv g_{\mathrm{Y}}/g_Z$, where g_Z is the coupling of the SM Z boson defined by $g_Z = 2M_Z/v$. Here $v = 246$ GeV is the SM Higgs vacuum expectation value. To simplify further, γ' and θ_{min} are chosen as independent parameters with the following definitions: $\tilde{g}_{\mathrm{B\text{-}L}} = \gamma' \cos\theta_{\mathrm{min}}$, $\tilde{g}_{\mathrm{Y}} = \gamma' \sin\theta_{\mathrm{min}}$. The γ' parameter measures the strength of the Z' boson coupling relative to that of the SM Z boson, while θ_{min} determines the mixing between the generators of the B-L and the weak hypercharge Y gauge groups. Specific values of γ' and θ_{min} correspond to Z' bosons in various models, as is shown in Table I for the three cases mentioned in this section.

TABLE I. Values for γ' and θ_{min} in the minimal Z' models corresponding to three specific Z' bosons: $Z'_{\mathrm{B\text{-}L}}$, Z'_χ and $Z'_{3\mathrm{R}}$. The SM weak mixing angle is denoted by θ_W.

	$Z'_{\mathrm{B\text{-}L}}$	Z'_χ	$Z'_{3\mathrm{R}}$
γ'	$\sqrt{\frac{5}{8}}\sin\theta_W$	$\sqrt{\frac{41}{24}}\sin\theta_W$	$\frac{5}{\sqrt{12}}\sin\theta_W$
$\cos\theta_{\mathrm{min}}$	1	$\sqrt{\frac{25}{41}}$	$\frac{1}{\sqrt{5}}$
$\sin\theta_{\mathrm{min}}$	0	$-\sqrt{\frac{16}{41}}$	$-\frac{2}{\sqrt{5}}$

For the minimal Z' models, the width depends on γ' and $\theta_{\min}$, and the interference with the SM Z/γ^* process is included. Couplings to hypothetical right-handed neutrinos and to W boson pairs are not included. Previous limits on the Z' mass versus couplings in the context of these models were set by the ATLAS experiment; the specific mass limit varies with γ'. For $\gamma' = 0.2$, the range of Z' mass limits at 95% C.L. corresponding to $\theta_{\min} \in [0, \pi]$ is 1.1 to 2.10 TeV [17].

C. Z^* bosons

One set of models proposes a solution to the SM hierarchy problem via the introduction of a new doublet of vector bosons: (Z^*, W^*) [7–10]. These are predicted to have masses near the weak scale, motivating the search at the LHC.

As a result of the tensor form of the coupling, the kinematics of the Z^* boson's decay to dileptons are different from that of a Z' boson [7], and there is no interference between this and the Z/γ^* process. To fix the Z^* boson's coupling strength to fermions, a model with quark-lepton universality is adopted [9,10]. The gauge coupling is chosen to be the same as in the SM $SU(2)$ group, and the scale of new physics is proportional to the mass of the new heavy boson. The model parameters are chosen such that the total and partial decay widths of the W^* are the same as those of the charged partner of the Z'_{SSM} boson (W'_{SSM}) with the same mass. The width of the Z^* resonance is 3.4% of its mass [10].

Previous ATLAS results exclude a Z^* with mass less than 2.20 TeV at 95% C.L. [17].

D. Graviton excitations in Randall-Sundrum models

Models with extra dimensions offer an alternative solution to the mass hierarchy problem in that the higher-dimensional Planck scale can be of the order of the electroweak scale. Among them, the Randall-Sundrum model [11] postulates the existence of one warped extra dimension. Specifically, the geometry of the original RS model contains two four-dimensional branes known as the TeV brane and the Planck brane, within a five-dimensional bulk. The extra dimension in the bulk is compactified, which leads to a Kaluza-Klein tower of excited states of the graviton. The particles of the SM are confined to the TeV brane, where due to warping the apparent strength of gravity is exponentially suppressed. Gravity originates on the Planck brane; gravitons are also located on the Planck brane, but can propagate in the bulk.

The RS model phenomenology is characterized by the mass of the lightest Kaluza-Klein excitation mode of the graviton known as G^*, and the ratio $k/\bar{M}_{\mathrm{Pl}}$, which defines the coupling strength of the G^* to SM particles. Here k is a scale that defines the warp factor of the extra dimension and $\bar{M}_{\mathrm{Pl}} = M_{\mathrm{Pl}}/\sqrt{8\pi}$ is the reduced Planck mass. The G^* in this model is expected to be narrow for values of $k/\bar{M}_{\mathrm{Pl}} < 0.2$. The intrinsic width of the particle is proportional to $(k/\bar{M}_{\mathrm{Pl}})^2$, and is 0.014% (5.8%) of the pole mass for $k/\bar{M}_{\mathrm{Pl}} = 0.01(0.2)$. A lower bound on $k/\bar{M}_{\mathrm{Pl}}$ of 0.01 is theoretically preferred [31], as it limits the new physics energy scale to be of the order of TeV, and less than 10 TeV. For values above $k/\bar{M}_{\mathrm{Pl}} \approx 0.1$ the compactification radius approaches the Planck length and is less motivated on theoretical grounds [31], as this theory does not incorporate quantum gravity.

The G^* is produced predominantly via quark-antiquark annihilation and gluon fusion, with decays to SM fermions or bosons. While the branching ratio to dileptons is low due to the spin-2 quantum numbers of the particle, the dilepton final state is nevertheless sensitive to new spin-2 resonances due to the clean final state.

Previous ATLAS results exclude a G^* with coupling $k/\bar{M}_{\mathrm{Pl}} = 0.1$ at 95% C.L. for masses less than 2.16 TeV [17], and the corresponding limit from CMS is 2.39 TeV [18].

E. Quantum black holes

In the context of models with extra dimensions, semiclassical black holes can be formed at a collider if the available energy is well above the higher-dimensional Planck scale [32,33]. Such black holes would then decay through Hawking radiation. Quantum (or nonthermal) black holes differ from these variants in that they lack a well-defined temperature or significant entropy. This inhibits thermal decays of black holes produced at a mass scale just above the (higher-dimensional) Planck scale, which in turn limits the number of particles in the final state [12]. For two-particle final states, it is interesting to look at the quantum gravity regime, where the threshold for QBH production, M_{th}, lies between the higher-dimensional Planck scale, and about 5 times this value [12,34,35]. The QBH decay is governed by the yet unknown theory of quantum gravity, but it is assumed that QBHs emit with equal strength all SM particle degrees of freedom. Provided the higher-dimensional Planck scale is not higher than a few TeV, QBHs could be observed at the LHC.

Production of QBHs can occur in the original RS model, and in the extra-dimensional model proposed by Arkani-Hamed, Dimopoulos, and Dvali (ADD) [36]. Both scenarios are considered in the model interpretation presented here. The ADD model postulates the existence of $n \geq 1$ flat additional spatial dimensions, commonly compactified with radius R. Only gravity propagates in these extra dimensions, with SM particles confined to a four-dimensional manifold. The threshold for QBH production in the ADD model is assumed to correspond to the higher-dimensional Planck scale. The analysis here was performed assuming $n = 6$, but the dependence of the resulting production limit on n is small.

The specific model [37] used to interpret the result of this article conserves color, electric charge, and total angular

momentum. Two QBHs states with zero charge produced via $q\bar{q}$ and gg have predicted branching ratios to each dilepton final state of 0.5% and 0.2%, respectively, assuming conservation of the global symmetries of lepton and baryon number. While the model parameters of Ref. [37] are considered in the context of ADD, one can take the five-dimensional ADD case to obtain an approximate RS model, which is what is used in the case of the RS model interpretation. In the RS model, the higher-dimensional Planck scale $\tilde{M}$ can be calculated from the G^* mass and $k/\bar{M}_{\mathrm{Pl}}$ as follows [12]:

$$\tilde{M} = \frac{M_{G^*}}{3.83 \times (k/\bar{M}_{\mathrm{Pl}})^{\frac{2}{3}}},$$

where also here the mass threshold for QBH production M_{th} is assumed to be equal to the higher-dimensional Planck scale.

Previous limits on the types of QBH production described in this article were set by the ATLAS experiment using final states with an energetic photon and a jet [38] as well as final states with an energetic lepton and a jet [39]. Previous limits also exist from the CMS experiment from a search dominated by multijet final states [40]. The ATLAS experiment has also set limits on the production of a different type of QBHs using dijet events [41,42]. While QBHs are not resonances, an increase in the dilepton production cross section near the black hole threshold is expected. The expected signal is therefore similar to that predicted by resonance models, and QBHs are thus referred to as resonances in the remainder of this article.

F. Minimal walking technicolor

Another solution to the hierarchy problem is to postulate that the Higgs boson is a composite particle, bound by a strong force called technicolor. Technicolor models use the new strong dynamics to break electroweak symmetry. These models predict the existence of new narrow technimeson resonances with masses of a few hundred GeV decaying to the dilepton final state. The interpretation used here is in the context of the minimal walking technicolor model [13–16], which predicts a composite Higgs boson having properties consistent, within current uncertainties, with the Higgs boson discovered at the LHC [5,6].

The MWT model used here is defined by the following parameters: the bare axial-vector and vector masses, M_A and M_V; the coupling of the spin-1 resonance to SM fermions $g/\tilde{g}$, where g is the coupling constant of the weak interaction and $\tilde{g}$ is the strength of the spin-1 resonance interaction; the S parameter obtained using the zeroth Weinberg sum rule used to constrain M_A and M_V; the Higgs boson mass m_H, and s, the coupling of the Higgs boson to composite spin-1 states. Here the S parameter and s are set according to the recommendation set forth in Ref. [43]: $S = 0.3$ and $s = 0$, while $m_H = 125$ GeV is used for the Higgs boson mass. The physical mass of about 125 GeV for the Higgs boson emerges after top quark corrections are taken into account [16].

This model predicts new particles in the form of technimeson triplets: $R_1^{0,\pm}$ and $R_2^{0,\pm}$. The R_1^0 and R_2^0 are produced by quark-antiquark annihilation and decay to dilepton final states via an intermediate Z/γ^* state. For each pair of values $(M_{R_1}, \tilde{g})$, the values of M_{R_2}, M_A, and M_V are unique. The widths and the mass difference of R_1 and R_2 vary strongly depending on the model parameters [44]. In this analysis, the model parameter $\tilde{g} = 2$ is used. Previous studies have shown [17] that the $m_{\ell\ell}$ distributions obtained with $\tilde{g} = 2$ are representative of those for all values of $\tilde{g}$ and M_A to which this analysis is currently sensitive. For this analysis, an $m_{\ell\ell}$ distribution accounting for contributions from both R_1 and R_2 is used. However, the magnitude of the mass difference between the two and the characteristics of the distribution are dependent on $\tilde{g}$ and M_A. For larger values of $\tilde{g}$ and small values of M_A, R_2 is broad with a reduced amplitude, and therefore does not contribute significantly to the signal shape.

Previous limits on this model were set by ATLAS on the bare axial mass, M_A, in the MWT model. For a value of the coupling parameter $\tilde{g} = 2$, M_A values less than 1.57 TeV were excluded at 95% C.L. [17].

III. ATLAS DETECTOR

The ATLAS detector [1] consists of an inner tracking detector system (ID) surrounded by a superconducting solenoid, electromagnetic and hadronic calorimeters, and a muon spectrometer (MS). Charged particles in the pseudorapidity[1] range $|\eta| < 2.5$ are reconstructed with the ID, which consists of layers of silicon pixel and microstrip detectors and a straw-tube transition-radiation tracker having coverage within $|\eta| < 2.0$. The ID is immersed in a 2 T magnetic field provided by the solenoid. The latter is surrounded by a hermetic calorimeter that covers $|\eta| < 4.9$ and provides three-dimensional reconstruction of particle showers. The electromagnetic calorimeter is a liquid argon sampling calorimeter, which uses lead absorbers for $|\eta| < 3.2$ and copper absorbers in the very forward region. The hadronic sampling calorimeter uses plastic scintillator tiles as the active material and iron absorbers in the region $|\eta| < 1.7$. In the region $1.5 < |\eta| < 4.9$, liquid argon is used as active material, with copper or/and tungsten absorbers. Outside the calorimeter, air-core toroids supply the magnetic field for the MS. There, three stations of

[1]ATLAS uses a right-handed coordinate system with its origin at the nominal interaction point in the center of the detector and the z axis along the beam pipe. The x axis points from the interaction point to the center of the LHC ring, and the y axis points upward. Cylindrical coordinates (r, ϕ) are used in the transverse plane, ϕ being the azimuthal angle around the beam pipe. The pseudorapidity is defined in terms of the polar angle θ as $\eta = -\ln\tan(\theta/2)$.

precision chambers allow the accurate measurement of muon track curvature in the region $|\eta| < 2.7$. The majority of these precision chambers are composed of drift tubes, while cathode strip chambers provide coverage in the inner stations of the forward region for $2.0 < |\eta| < 2.7$. Additional muon chambers installed between the inner and middle stations of the forward region and commissioned prior to the 2012 run improve measurements in the transition region of $1.05 < |\eta| < 1.35$ where the outer stations have no coverage. Muon triggering is possible in the range $|\eta| < 2.4$, using resistive-plate chambers in the central region and thin-gap chambers in the forward region. A three-level trigger system [45] selects events to be recorded for off-line analysis.

IV. DATA SAMPLE

The events in the data set were collected during periods with stable beams and all relevant subsystems operational. The pp collision data recorded between April and December 2012 at $\sqrt{s} = 8$ TeV amount to 20.3 fb^{-1} in the dielectron channel and 20.5 fb^{-1} in the dimuon channel.

In the dielectron channel, events are triggered by the presence of two energy deposits ("clusters") in the electromagnetic calorimeter, one with transverse momentum (p_T) threshold of $p_T > 35$ GeV, and the other with $p_T > 25$ GeV. The shower profiles are required to be consistent with those expected for electromagnetic showers [46]. This trigger is preferred over a dedicated dielectron trigger, which incorporates tracking information, because it is advantageous in the estimation of the data-driven background, as explained in Sec. VIII. In the dimuon channel, events are triggered by at least one of two single-muon triggers with transverse momentum thresholds of $p_T > 24$ GeV or $p_T > 36$ GeV with an additional requirement that the muon candidate be isolated (see Sec. VI) for the former case.

V. SIMULATED SAMPLES

Expected signal and background yields, with the exception of certain data-driven background estimates, are evaluated with simulated Monte Carlo (MC) samples and normalized using the highest-order cross-section predictions available in perturbation theory.

The sample used to model the Drell-Yan ($q\bar{q} \to Z/\gamma^* \to \ell^+\ell^-$) background is generated at next-to-leading order (NLO) using POWHEG [47] and the CT10 PDF [48], with PYTHIA 8 [49] to model parton showering and hadronization. For this and all other samples, the final-state photon radiation (FSR) is handled by PHOTOS [50], and the interaction of particles with the detector and its response are modeled using a full ATLAS detector simulation [51] based on GEANT4 [52]. The Z/γ^* differential cross section with respect to mass has been calculated at next-to-next-to-leading-order (NNLO) perturbative QCD (pQCD) using FEWZ [53,54] with the MSTW2008NNLO PDF [55]. The calculation includes NLO electroweak (EW) corrections beyond FSR, as well as a contribution from the irreducible, nonresonant photon-induced (PI) background, $\gamma\gamma \to \ell^+\ell^-$. The PI contribution is estimated using the MRST2004qed PDF [56] at leading order, by taking an average of the predictions obtained under the current and constituent quark mass schemes. Differences between the average and the individual results from those schemes are used to assign the uncertainty on this additive correction. The PI corrections were verified by SANC [57,58]. An additional small correction arises from single boson production in which the final-state charged lepton radiates a real W or Z boson. This was estimated using MADGRAPH 5 [59], following the prescription outlined in Ref. [60]. A mass-dependent K factor used to scale the Z/γ^* background samples is obtained from the ratio of the calculated NNLO pQCD cross section, with additional EW, PI, and real W/Z corrections, to the cross section from the POWHEG sample. The values of the K factors as evaluated at dilepton masses of 1, 2, and 3 TeV are 1.07, 1.10, and 1.14, respectively.

Other important backgrounds are due to diboson (WW, WZ, and ZZ) and top quark production. The diboson processes are generated with HERWIG [61,62] using the CTEQ6L1 PDF [63]. The diboson cross sections are known to NLO with an uncertainty of 5%, and the values used are 57 pb (WW), 21 pb (WZ), and 7.4 pb (ZZ), as calculated with MCFM [64]. Backgrounds from $t\bar{t}$ and from single top production in association with a W boson are modeled with MC@NLO [65–67] with HERWIG using the CT10 PDF. The $t\bar{t}$ cross section is $\sigma_{t\bar{t}} = 253^{+13}_{-15}$ pb for a top quark mass of 172.5 GeV. This is calculated at NNLO in QCD including resummation of next-to-next-to-leading logarithmic soft gluon terms with TOP++2.0 [68–73]. The PDF and α_S uncertainties on the $t\bar{t}$ cross section are calculated using the PDF4LHC prescription [74] with the MSTW2008 68% C.L. NNLO [55,75], CT10 NNLO [48,76], and NNPDF2.3 5f FFN [77] PDF error sets added in quadrature to the scale uncertainty. Varying the top quark mass by ± 1 GeV leads to an additional systematic uncertainty of $+8$ and -7 pb, which is also added in quadrature. The single top background in association with a W boson has a cross section of $\sigma_{Wt} = 22.4 \pm 1.5$ pb [78]. Given that the Wt contribution is small compared to the $t\bar{t}$ cross section, an overall uncertainty of 6% is estimated on the top quark background. The simulated top quark samples are statistically limited at high invariant mass, and the expected number of events as a function of $m_{\ell\ell}$ is therefore extrapolated into this region using fits. A number of fits to the invariant mass distribution are carried out, exploring various fit ranges as well as the two fit functions $y(x) = p_1 x^{p_2 + p_3 \log x}$ and $y(x) = p_1/(x + p_2)^{p_3}$, where y represents the expected yield and $x = m_{\ell\ell}$. The mean and rms of these fits are used as the background contribution and its uncertainty, respectively. Background contributions from

TABLE II. Overview of simulated samples used.

Process	Generator	Parton shower	PDF
Drell-Yan	POWHEG	PYTHIA 8.162	CT10
Diboson	HERWIG++ 2.5.2	HERWIG 6.520	CTEQ6L1
$t\bar{t}$, Wt	MC@NLO 4.06	HERWIG 6.520	CT10
Z'	PYTHIA 8.165	PYTHIA 8.165	MSTW2008LO
G^*	PYTHIA 8.160	PYTHIA 8.160	CTEQ6L
Z^*	CALCHEP 4.5.1	PYTHIA 8.165	MSTW2008LO
MWT	MADGRAPH 5	PYTHIA 8.165	MSTW2008LO
QBH	QBH 1.05	PYTHIA 8.165	CT10

events with jets or photons in the final state that pass the electron selection criteria are determined using the data, as explained in Sec. VIII. In the muon channel this background is negligible. In order to avoid double counting, the simulated samples in the electron channel are filtered for the presence of two electrons.

An overview of the simulated MC signal and background samples is given in Table II.

Simulated signal processes for the Z' models are obtained by reweighting PYTHIA 8 Drell-Yan samples to the shape of the resonance. The same technique is used for MWT signals, and the shape of the resonance is obtained using MADGRAPH 5. A reweighting procedure is also used for Z^* and G^* signals, but it is applied to dedicated samples generated with CALCHEP [79] in the case of Z^*, and with PYTHIA 8 in the case of G^*. For the QBH signals, samples are generated for each assumed energy threshold (M_{th}) using the QBH [80] generator. The MSTW2008LO PDF [55] is used for all signal samples, except the G^*, which uses the CTEQ6L PDF [63]. The ratio of the NNLO pQCD cross section calculated with FEWZ without the additional EW, PI, and real W/Z corrections to the cross section from the PYTHIA 8 sample is used to determine a mass-dependent K factor for the signal samples. The values of the K factors as evaluated at dilepton masses of 1, 2, and 3 TeV are 1.22, 1.16, and 1.16, respectively. The additional EW and real W/Z corrections are not applied to the signal samples because the dominant EW corrections depend on the W and Z boson couplings of the new particle, and are therefore model dependent. The PI contribution is nonresonant and thus only contributes to the background. No K factor is applied to the leading-order Z^* and QBH cross sections. This is due to the different coupling of the Z^* to fermions, and the unknown gravitational interaction. For G^*, a NLO K factor was provided by the authors of Refs. [81–83], using CTEQ6L, which is the same PDF used in the simulation of the signal.

VI. LEPTON RECONSTRUCTION

Electron candidates are formed from clusters of cells reconstructed in the electromagnetic calorimeter with an associated well-reconstructed ID track. The track and the cluster must satisfy a set of identification criteria [46] that are optimized for high pile-up[2] conditions. These criteria require the shower profiles to be consistent with those expected for electrons and impose a minimum requirement on the amount of transition radiation. In addition, to suppress background from photon conversions, a hit in the first layer of the pixel detector is required if an active pixel layer is traversed. The electron's energy is obtained from the calorimeter measurements and its direction from the associated track.

At transverse energies (E_T) relevant to this search, the calorimeter energy resolution is measured in data to be 1.2% for electrons in the central region ($|\eta| < 1.37$) and 1.8% in the forward region ($1.52 < |\eta| \leq 2.47$) [84]. For dielectron masses above 200 GeV, the mass resolution is below 2% over the entire η range.

To suppress background from misidentified jets, isolated electrons are selected. A limit is placed on the energy corrected for transverse shower leakage and pile-up contained in a cone of radius $\Delta R = 0.2$ surrounding the electron candidate in the (η, ϕ) plane: $\Delta R = \sqrt{(\Delta\eta)^2 + (\Delta\phi)^2}$. For the leading (highest-p_T) electron candidate this energy is required to be less than $0.007 \times E_T + 5.0$ GeV, while for the subleading electron candidate a requirement of less than $0.022 \times E_T + 6.0$ GeV is used. These requirements have been optimized to maintain a high selection efficiency of ≈99% for each electron candidate. The difference in the isolation selection for the leading and subleading electrons takes into account the different energy losses due to bremsstrahlung.

Muon tracks are first reconstructed [85,86] separately in the ID and in the MS. The two tracks are then matched and a combined fit is performed using ID and MS hits, taking into account the effects of multiple scattering and energy loss in the calorimeters. The momentum is taken from the combined fit. Each muon is required to have a minimum number of hits in each of the ID components. To obtain optimal momentum resolution, at least one selected muon is required to have at least three hits in each of three stations of the MS, or, for muons in the very forward region, at least two hits in the cathode strip chambers and at least three hits in the middle and outer MS stations. At least one hit in each of two layers of the trigger chambers is also required. These muons are referred to as three-station muons, and have p_T resolution at 1 TeV ranging from 19% to 32%, depending on η. In the very forward region of the MS, the hit requirement in the inner station corresponds to at least two hits in the cathode strip chambers.

In addition to three-station muons, the best remaining muon candidates in the central region of the MS ($|\eta| < 1.05$) with at least five precision hits in each of the inner and outer stations are selected, and are referred to

[2]Multiple pp collisions occurring in the same or neighboring bunch crossings.

as two-station muons. These two-station muons are required to have at least one hit in one layer of the trigger chambers, and they have slightly worse p_T resolution than the three-station muons.

Residual misalignments of the muon detectors, which could cause a degradation of the momentum resolution, were studied with collision data in which the muons traversed overlapping sets of muon chambers. The effects of these misalignments and the intrinsic position resolution are included in the simulation. Muon candidates passing through chambers where the alignment quality does not allow a reliable momentum measurement at high p_T are rejected.

For each three-station (two-station) muon, the difference between the stand-alone momentum measurements from the ID and MS must not exceed 5 (3) times the sum in quadrature of the stand-alone uncertainties. To suppress background from cosmic rays, the muons are also required to satisfy requirements on the track impact parameters with respect to the primary vertex of the event. The impact parameter along the beam axis is required to be within 1 mm, and the transverse impact parameter is required to be within 0.2 mm. The primary vertex of the event is defined as the reconstructed vertex consistent with the beam spot position with the highest $\sum p_T^2$. The sum includes the p_T^2 of all tracks associated with the primary vertex. At least three associated tracks are required, each with p_T above 0.4 GeV. To reduce the background from misidentified jets, each muon is required to be isolated such that $\Sigma p_T(\Delta R < 0.3)/p_T(\mu) < 0.05$, where $\Sigma p_T(\Delta R < 0.3)$ is the scalar sum of the p_T of all other tracks with $p_T > 1$ GeV within a cone of radius $\Delta R = 0.3$ around the direction of the muon.

VII. EVENT SELECTION

Events are required to have at least one reconstructed primary vertex.

For the dielectron channel, at least two reconstructed electron candidates within $|\eta| < 2.47$ are required. In each event, the leading electron and the subleading electron must satisfy $E_T > 40$ GeV and $E_T > 30$ GeV, respectively. The transition region between the central and forward regions of the calorimeters, in the range $1.37 \leq |\eta| \leq 1.52$, exhibits degraded energy resolution and is therefore excluded. Because of possible charge misidentification, an opposite-charge requirement is not placed on electron candidates. Charge misidentification can occur either due to bremsstrahlung, or due to the limited momentum resolution of the ID at very high p_T.

The product of acceptance and efficiency ($A \times \epsilon$) is defined as the fraction of simulated candidate events that pass the dilepton event selection requirement in the $m_{\ell\ell}$ search region 128 GeV $< m_{\ell\ell} <$ 4500 GeV, out of those generated with a Born level dilepton mass greater than 60 GeV. Figure 1 shows $A \times \epsilon$ as a function of the Z'_{SSM} pole mass for both channels. Using the described search criteria, $A \times \epsilon$ in the dielectron channel is found to be 71% for a Z'_{SSM} pole mass of 2 TeV. For low values of the Z'_{SSM} pole mass, $A \times \epsilon$ rises due to kinematic selection requirements. It drops again at high pole mass because the strong decrease of the parton luminosity at high momentum transfer enhances the relative fraction of events in the low-mass tail of the spectrum arising from off-shell Z'_{SSM} production.

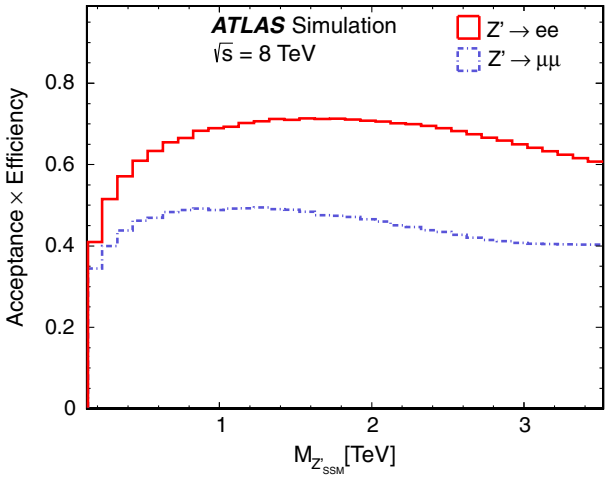

FIG. 1 (color online). Product of acceptance and efficiency for the dielectron (upper distribution) and dimuon (lower distribution) selections as a function of the Z'_{SSM} pole mass.

Muons passing the reconstruction criteria are required to satisfy $p_T > 25$ GeV and are used to build opposite-charge muon pairs. If two opposite-charge muons passing the three-station selection are found, they are used to make the pair and the event is said to pass the "primary dimuon selection." If no primary dimuon candidate is found, pairs are built with one three-station muon and a two-station muon of opposite charge. Events with such pairs are said to pass the "secondary dimuon selection." For both selections, if more than one dimuon candidate is found in an event, the one with the highest transverse momentum scalar sum is selected. In the case of a Z'_{SSM} of mass 2 TeV, $A \times \epsilon$ in the dimuon channel is estimated to be 46%, as can be seen in Fig. 1. The contribution of the primary (secondary) dimuon selection is about 42% (4%) at 2 TeV. Due to the stringent requirements placed on the number and distribution of hits required in the MS, which ensure good momentum resolution at large $m_{\ell\ell}$, the $A \times \epsilon$ for the dimuon channel is lower compared to the dielectron channel.

VIII. DATA-DRIVEN BACKGROUNDS

As mentioned above, background contributions from events with jets or photons in the final state that pass the electron selection criteria are determined using the data. This includes contributions from dijet, heavy-flavor quarks, and γ + jet production referred to hereafter as the dijet

background. Additional contributions are due to $W+$jets processes and top quark production with $W+$jets final states referred to hereafter as $W+$jets background.

The probability that a jet is misidentified as an electron (the "fake rate") is determined as a function of E_T and η using background-enriched data samples. These samples are recorded using several inclusive jet triggers with E_T thresholds in the range 25–360 GeV. In each of these samples, the fake rate f_1 (f_2) is calculated as the fraction of leading (subleading) electron candidates that pass the nominal electron identification and isolation requirements ("tight"), with respect to the entire sample of "loose" electron candidates. The loose candidates satisfy only a subset of the nominal electron identification criteria. However, this subset has to be stricter than the trigger requirements imposed on a single object. To avoid bias due to a real electron contribution from W decays or the Drell-Yan process, events are vetoed in the following cases: if the missing transverse momentum is larger than 25 GeV, if they contain two identified electrons satisfying strict criteria, or if they contain two electrons satisfying less strict criteria but with an invariant mass between 71 and 111 GeV. A weighted average of the fake rates obtained from the jet samples is then calculated. The values of the fake rates are around 10%. They are not strongly E_T dependent, but are smaller at central pseudorapidities and increase to as high as 20% for $2.4 < |\eta| < 2.47$.

In addition to the fake rate, the probability r_1 (r_2) that a real electron in the sample of loose electrons satisfies the nominal electron identification and leading (subleading) isolation requirements is used in evaluating this background. This probability is computed from MC simulation. Potential differences between data and simulated samples in lepton identification and isolation efficiencies are accounted for by applying scale factors to the simulation, which are generally close to unity. The values for r_1 and r_2 are well above 90% for all E_T and η.

A system of equations is used to solve for the unknown true contribution to the background from events with one or more fake electrons. The relation between the number of true paired objects N_{ab}, with $E_{\mathrm{T}}^a > E_{\mathrm{T}}^b$ and $a, b \in \{R, F\}$, and the number of measured pairs in the triggered sample N_{xy}, with $x, y \in \{T, L\}$, can be written as

$$\begin{pmatrix} N_{TT} \\ N_{TL} \\ N_{LT} \\ N_{LL} \end{pmatrix} = \begin{pmatrix} r_1 r_2 & r_1 f_2 & f_1 r_2 & f_1 f_2 \\ r_1(1-r_2) & r_1(1-f_2) & f_1(1-r_2) & f_1(1-f_2) \\ (1-r_1) r_2 & (1-r_1) f_2 & (1-f_1) r_2 & (1-f_1) f_2 \\ (1-r_1)(1-r_2) & (1-r_1)(1-f_2) & (1-f_1)(1-r_2) & (1-f_1)(1-f_2) \end{pmatrix} \begin{pmatrix} N_{RR} \\ N_{RF} \\ N_{FR} \\ N_{FF} \end{pmatrix}. \quad (1)$$

The subscripts R and F refer to real electrons and fakes (jets), respectively. The subscript T refers to electrons that pass the tight selection. The subscript L corresponds to electrons that pass the loose requirements described above but fail the tight requirements.

The background is given as the part of N_{TT}, the number of pairs where both objects are reconstructed as signal-like, originating from a pair of objects with at least one fake:

$$N_{TT}^{\mathrm{Dijet\&}W+\mathrm{jets}} = r_1 f_2 N_{RF} + f_1 r_2 N_{FR} + f_1 f_2 N_{FF}. \quad (2)$$

The true paired objects on the right-hand side of Eq. (2) can be expressed in terms of measurable quantities (N_{TT}, N_{TL}, N_{LT}, N_{LL}) by inverting the matrix in Eq. (1).

The dijet background in the dimuon sample is evaluated from data by reversing the requirement that muons pass the track isolation requirement based on the variable $\Sigma p_T(\Delta R < 0.3)/p_T$. The method is further described in Ref. [87]. The contribution of the dijet background in the dimuon channel is negligible, as is the background from cosmic rays.

IX. SYSTEMATIC UNCERTAINTIES

The treatment of systematic uncertainties in this analysis is simplified by the fact that the backgrounds are normalized to the data in the region of the Z peak. This procedure makes the analysis insensitive to the uncertainty on the measurement of the integrated luminosity as well as other mass-independent systematic uncertainties. A mass-independent systematic error of 4% is assigned to the signal expectation due to the uncertainty on the Z/γ^* cross section in the normalization region. This uncertainty is due to the PDF and α_S uncertainties obtained from the 90% C.L. MSTW2008NNLO PDF error set, using the program VRAP [88] in order to calculate the NNLO Drell-Yan cross section in the normalization region. In addition, scale uncertainties are estimated by varying the renormalization and factorization scales simultaneously up and down by a factor of 2, also using VRAP.

Mass-dependent systematic uncertainties include theoretical and experimental effects on the signal and background. These uncertainties are correlated across all $m_{\ell\ell}$ bins in the search region. The mass-dependent theoretical uncertainties are applied to the Z/γ^* background expectation only. In general, theoretical uncertainties are not applied to the signal. However, the mass dependence of the

PDF uncertainty due to acceptance variations was checked and found to be negligible. It is assumed that the experimental uncertainties are fully correlated between the signal and all types of background. In the statistical analysis, all systematic uncertainties estimated to have an impact $< 3\%$ on the expected number of events for all values of $m_{\ell\ell}$ are neglected, as they have negligible impact on the results of the search.

The combined uncertainty on the Z/γ^* background due to PDF ("PDF variation") and α_S is obtained from the 90% C.L. MSTW2008NNLO PDF error set, using VRAP in order to calculate the NNLO Drell-Yan cross section as a function of $m_{\ell\ell}$. The resulting uncertainties at dilepton masses of 2 and 3 TeV are given in Tables III and IV, respectively. An additional uncertainty is assigned to take into account potential differences between modern PDFs at the same $\alpha_S = 0.117$: MSTW2008NNLO, CT10NNLO, NNPDF2.3 [77], ABM11 [89], and HERAPDF1.5 [90]. Of these, only the central values for ABM11 fall outside of the MSTW2008NNLO PDF's uncertainty band. Thus, an envelope of the latter uncertainty and the ABM11 central value is formed with respect to the central value of the MSTW PDF. The 90% C.L. uncertainty from MSTW is subtracted in quadrature from this envelope, and the remaining part, which is only nonzero when the ABM11 central value is outside the MSTW2008NNLO PDF uncertainty, is quoted as "PDF choice." Scale uncertainties are estimated by varying the renormalization and factorization scales simultaneously up and down by a factor of 2, also using VRAP. The resulting maximum variations are taken as uncertainties and are less than 3%. The uncertainty on the PI correction is taken as half the difference between the predictions obtained under the current and constituent quark mass schemes, as discussed in Sec. V. In addition, a systematic uncertainty is attributed to EW corrections for both channels, corresponding to the difference in the theoretical calculation between FEWZ and SANC.

TABLE III. Summary of systematic uncertainties on the expected numbers of events at a dilepton mass of $m_{\ell\ell} = 2$ TeV, where N/A indicates that the uncertainty is not applicable. Uncertainties $< 3\%$ for all values of m_{ee} or $m_{\mu\mu}$ are neglected in the respective statistical analysis.

	Dielectrons		Dimuons	
Source ($m_{\ell\ell} = 2$ TeV)	Signal	Background	Signal	Background
Normalization	4%	N/A	4%	N/A
PDF variation	N/A	11%	N/A	12%
PDF choice	N/A	7%	N/A	6%
α_s	N/A	3%	N/A	3%
Electroweak correction	N/A	2%	N/A	3%
Photon-induced correction	N/A	3%	N/A	3%
Beam energy	<1%	3%	<1%	3%
Resolution	<3%	<3%	<3%	3%
Dijet and W + jets	N/A	5%	N/A	N/A
Total	4%	15%	4%	15%

TABLE IV. Summary of systematic uncertainties on the expected numbers of events at a dilepton mass of $m_{\ell\ell} = 3$ TeV, where N/A indicates that the uncertainty is not applicable. Uncertainties $< 3\%$ for all values of m_{ee} or $m_{\mu\mu}$ are neglected in the respective statistical analysis.

	Dielectrons		Dimuons	
Source ($m_{\ell\ell} = 3$ TeV)	Signal	Background	Signal	Background
Normalization	4%	N/A	4%	N/A
PDF variation	N/A	30%	N/A	17%
PDF choice	N/A	22%	N/A	12%
α_s	N/A	5%	N/A	4%
Electroweak correction	N/A	4%	N/A	3%
Photon-induced correction	N/A	6%	N/A	4%
Beam energy	<1%	5%	<1%	3%
Resolution	<3%	<3%	<3%	8%
Dijet and W + jets	N/A	21%	N/A	N/A
Total	4%	44%	4%	23%

On the experimental side, a systematic effect common to both channels is due to an uncertainty of 0.65% on the beam energy [91]. The effect on the background cross section was evaluated for the dominant Z/γ^* background only, and it can be as high as 5% at high dilepton masses. For the signals considered here, the effect of this uncertainty on $A \times \epsilon$ is negligible ($<1\%$).

In the dielectron channel, the systematic uncertainty is dominated by the determination of background contributions with jets faking electrons in the final state, mainly dijet and W + jets processes. In order to derive this uncertainty, the method described above was altered by assuming $r_1 = r_2 = 1$. This second "matrix method" leads to a simplification of the matrix in Eq. (1), but also necessitates the use of MC corrections for the identification and isolation inefficiencies of real electrons. Large corrections from MC simulation can be avoided in a third matrix method where objects in the background-enriched sample fail the requirement on the matching between track and cluster, instead of the full identification and isolation requirements.

In addition to the standard background-enriched sample recorded using the jet triggers, two alternative background-enriched samples are obtained using a "tag and probe" technique on the jet-triggered sample and the sample triggered by electromagnetic objects. Here the choice of an electromagnetic-object trigger that is looser than a dedicated electron trigger (see Sec. IV) leads to an enlarged sample. The background-enriched sample of probes is obtained by selecting a jetlike tag and a probe with the same charge, among other requirements, in order to suppress real electron contamination. Finally, the default method and the two additional matrix methods are each used in conjunction with the default sample and the two different background-enriched samples, leading to nine different background estimates. In the $m_{\ell\ell}$ search region, the maximum deviation of the eight alternative estimates

from the default background estimate is 18% and is taken as a systematic uncertainty at all values of $m_{\ell\ell}$.

Furthermore, the different requirements used to suppress real electron contamination in the default fake-rate calculation are varied. The largest deviations, about 5%, occur when the value of the missing energy requirement is changed. The statistical uncertainty on the fake rates results in an uncertainty on the background of at most 5%.

Another systematic uncertainty can arise if fake rates are different for the various processes contributing to the background, and if the relative contributions of these processes in the data samples from which the fake rates are measured and in the data sample to which the fake rates are applied are different. Jets originating from bottom quarks have a higher fake rate than jets originating from light-quark jets, but the effect of this is negligible as the number of b jets is small and similar in both samples. As an additional check, the background is recalculated using all nine methods discussed above, but with separate fake rates for different background processes. The mean of these nine methods is in agreement with the background estimate from the default method.

Thus, adding the different sources of uncertainty in quadrature, an overall systematic uncertainty of 20% is assigned to the dijet and $W+$jets background. At low invariant masses there is an additional uncertainty due to the statistical uncertainty from the sample to which the fake rates are applied. At high invariant masses this component is replaced by a systematic uncertainty due to the background extrapolation into this region. The extrapolation is done in the same way as for the top quark background (see Sec. V) and dominates the uncertainty on the dijet and $W+$jets background contribution at the highest invariant masses.

Experimental systematic uncertainties from the electron reconstruction and identification efficiencies, as well as from the energy calibration and resolution are neglected, as they alter the expected number of events by less than 3%.

For the dimuon channel, the combined uncertainty on the trigger and reconstruction efficiencies is negligible. Inefficiencies may occur for muons with large energy loss due to bremsstrahlung in the outer parts of the calorimeter, interfering with muon reconstruction in the MS. However, such events are rare and the corresponding systematic uncertainty is negligible over the entire mass range considered. This is an improvement on previous ATLAS publications [17], which used a very conservative, and much larger, estimate: 6% at 2 TeV. In addition, the uncertainty on the resolution due to residual misalignments in the MS propagates to a change in the steeply falling background shape at high dilepton mass and in the width of signal line shape. The potential impact of this uncertainty on the background estimate reaches 3% at 2 TeV and 8% at 3 TeV. The effect on the signal is negligible. As for the dielectron channel, the momentum scale uncertainty has negligible impact in the dimuon channel search.

Mass-dependent systematic uncertainties that change the expected number of events by at least 3% anywhere in the $m_{\ell\ell}$ distribution are summarized in Tables III and IV for dilepton invariant masses of 2 and 3 TeV, respectively.

X. COMPARISON OF DATA AND BACKGROUND EXPECTATIONS

The observed invariant mass distributions m_{ee} and $m_{\mu\mu}$ are compared to the expectation from SM backgrounds after final selection. To make this comparison, the sum of all simulated backgrounds, with the relative contributions fixed according to the respective cross sections, is scaled such that the result agrees with the observed number of data events in the 80–110 GeV normalization region, after subtracting the data-driven background in the case of the electron channel. The scale factors obtained with this procedure are 1.02 in the dielectron channel and 0.98 in the dimuon channel. It is this normalization approach that

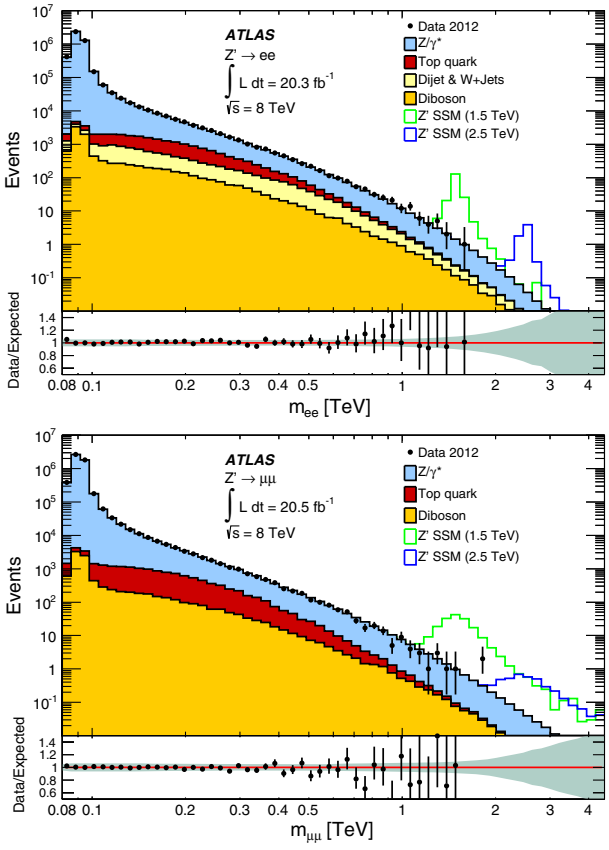

FIG. 2 (color online). Dielectron (top) and dimuon (bottom) invariant mass ($m_{\ell\ell}$) distributions after event selection, with two selected Z'_{SSM} signals overlaid, compared to the stacked sum of all expected backgrounds, and the ratios of data to background expectation. The bin width is constant in log $m_{\ell\ell}$. The green band in the ratio plot shows the systematic uncertainties described in Sec. IX.

TABLE V. The numbers of expected and observed events in the dielectron (top) and dimuon (bottom) channel in bins of the invariant mass $m_{\ell\ell}$. The region 80–110 GeV is used to normalize the total background to the data. The errors quoted are the combined statistical and systematic uncertainties.

m_{ee} [GeV]	110–200	200–400	400–800	800–1200	1200–3000	3000–4500
Z/γ^*	122000 ± 7000	14000 ± 800	1320 ± 70	70 ± 5	10.0 ± 1.0	0.008 ± 0.004
Top	8200 ± 700	2900 ± 500	200 ± 80	3.1 ± 0.8	0.16 ± 0.08	< 0.001
Diboson	1880 ± 90	680 ± 40	94 ± 5	5.9 ± 0.4	1.03 ± 0.06	< 0.001
Dijet & W + jet	3900 ± 800	1290 ± 320	230 ± 70	9.0 ± 2.3	0.9 ± 0.5	0.002 ± 0.004
Total	136000 ± 7000	18800 ± 1000	1850 ± 120	88 ± 5	12.1 ± 1.1	0.011 ± 0.005
Observed	136200	18986	1862	99	9	0

$m_{\mu\mu}$ [GeV]	110–200	200–400	400–800	800–1200	1200–3000	3000–4500
Z/γ^*	111000 ± 8000	11000 ± 1000	1000 ± 100	49 ± 5	7.3 ± 1.1	0.034 ± 0.022
Top	7100 ± 600	2300 ± 400	160 ± 80	3.0 ± 1.7	0.17 ± 0.15	< 0.001
Diboson	1530 ± 180	520 ± 130	64 ± 16	4.2 ± 2.1	0.69 ± 0.30	0.0024 ± 0.0019
Total	120000 ± 8000	13700 ± 1100	1180 ± 130	56 ± 6	8.2 ± 1.2	0.036 ± 0.023
Observed	120011	13479	1122	49	8	0

allows the mass-independent uncertainties to cancel in the statistical analysis.

Figure 2 depicts the $m_{\ell\ell}$ distributions for the dielectron and dimuon final states. The bin width of the histograms is constant in $\log m_{\ell\ell}$, chosen such that a possible signal peak spans multiple bins and the shape is not impacted by statistical fluctuations at high mass. The shaded band in the ratio inset represents the systematic uncertainties described in Sec. IX. Figure 2 also displays the expected Z'_{SSM} signal for two mass hypotheses. Table V shows the number of data events and the estimated backgrounds in several bins of reconstructed dielectron and dimuon invariant mass above 110 GeV. The number of observed events in the normalization region is 4,257,744 in the dielectron channel and 5,075,739 in the dimuon channel. The higher yield in the normalization region for the dimuon channel, despite the lower $A \times \epsilon$ at higher masses as displayed in Fig. 1, is due to the higher E_T cuts on the electrons. This reduces the yield in the dielectron channel in the region of the Z peak. The dilepton invariant mass distributions are well described by the predictions from SM processes.

XI. STATISTICAL ANALYSIS

The data are compared to the background expectation in the search region. The comparison is performed by means of signal and background templates [92,93] that provide the expected yield of events ($\bar{n}$) in each $m_{\ell\ell}$ bin. The dependence of the resonance width on the coupling strength is taken into account in the signal templates. The coupling to hypothetical right-handed neutrinos and to W boson pairs is neglected in the Z' search. Interference of the Z' signal with the Drell-Yan background is taken into account in the minimal Z' models interpretation framework only. When interference is not taken into account, $\bar{n}$ is given by $\bar{n} = n_X(\lambda, \boldsymbol{\nu}) + n_{Z/\gamma^*}(\boldsymbol{\nu}) + n_{\mathrm{obg}}(\boldsymbol{\nu})$, where n_X represents the number of events produced by the decay of a new resonance, X ($X = Z'$, Z^*, G^*, $M_{\mathrm{th}}, R_{1,2}$), and n_{Z/γ^*} and n_{obg} are the number of Z/γ^* (Drell-Yan) and other backgrounds events, respectively. The symbol λ represents the parameter of interest in the model, and $\boldsymbol{\nu}$ is the set of Gaussian-distributed nuisance parameters incorporating systematic uncertainties. When interference effects are included, $\bar{n} = n_{X+Z/\gamma^*}(\lambda, \boldsymbol{\nu}) + n_{\mathrm{obg}}(\boldsymbol{\nu})$, where n_{X+Z/γ^*} is the number of signal plus Z/γ^* events and X is the Z' boson in the minimal models interpretation. A binned likelihood function is employed for the statistical analysis. The likelihood function is defined as the product of the Poisson probabilities over all mass bins in the search region,

$$\mathcal{L}(\lambda, \boldsymbol{\nu}) = \prod_i^{N_{\mathrm{bins}}} \frac{e^{-\bar{n}_i} \bar{n}^{d_i}}{d_i!} G(\boldsymbol{\nu}).$$

The symbol d_i corresponds to the observed number of events in bin i of the $m_{\ell\ell}$ distribution and $G(\boldsymbol{\nu})$ represents the Gaussian functions for the set of nuisance parameters $\boldsymbol{\nu}$.

The significance of a signal is summarized by a p value, the probability of observing an excess at least as signal-like as the one observed in data, assuming the null hypothesis. The outcome of the search is ranked using a log-likelihood ratio (LLR) test statistic, using a Z'_{SSM} template assuming no interference. Explicitly,

$$\mathrm{LLR} = -2 \ln \frac{\mathcal{L}(\mathrm{data}|\hat{n}_{Z'}, \hat{M}_{Z'}, \hat{\boldsymbol{\nu}})}{\mathcal{L}(\mathrm{data}|(\hat{n}_{Z'} = 0), \hat{\hat{\boldsymbol{\nu}}})},$$

where $\hat{n}_{Z'}$ and $\hat{M}_{Z'}$ are the best-fit values for the Z' normalization and the Z' mass. The nuisance parameters that maximize the likelihood $\mathcal{L}$ given the data are represented by $\hat{\boldsymbol{\nu}}$ and $\hat{\hat{\boldsymbol{\nu}}}$, assuming in the numerator that a Z' signal is present, and in the denominator that no signal is present. The LLR is scanned as a function of Z' cross section and $M_{Z'}$ over the full considered mass range. This approach naturally

includes the trials factor, which accounts for the probability of observing an excess anywhere in the search region. The observed p values for the dielectron and dimuon samples are 27% and 28%, respectively.

In the absence of a signal, upper limits on the number of events produced by the decay of a new resonance are determined at 95% C.L. The same Bayesian approach [94] is used in all cases, with a uniform positive prior probability distribution for the parameter of interest. When interference is not taken into account, the parameter of interest is the signal cross section times branching fraction (σB). When interference effects are included the coupling strength is chosen as the parameter of interest, with a prior that is flat in the coupling strength to the fourth power. The most likely number of signal events, and the corresponding confidence intervals, are determined from the binned likelihood function defined above. The product of acceptance and efficiency for the signal as a function of mass is different for each model considered due to different angular distributions, boosts, and line shapes. This is propagated into the expectation. The dependence of the likelihood on the nuisance parameters is integrated out using the Markov Chain Monte Carlo method [94].

The expected exclusion limits are determined using simulated pseudoexperiments with only SM processes by evaluating the 95% C.L. upper limits for each pseudoexperiment for each fixed value of the resonance pole mass, M_X. The median of the distribution of limits is chosen to represent the expected limit. The ensemble of limits is also used to find the 68% and 95% envelopes of the expected limits as a function of M_X.

The combination of the dielectron and dimuon channels is performed under the assumption of lepton universality. For each source of systematic uncertainty, the correlations across bins, as well as the correlations between signal and background, are taken into account.

XII. MODEL INTERPRETATION AND RESULTS

As no evidence for a signal is observed, limits are set in the context of the physics models introduced in Sec. II. For all but the minimal Z' models, limits are set on σB versus the resonance mass. The predicted σB is used to derive limits on the resonance mass for each model. Table VI lists the predicted σB values for a few resonance masses and model parameters. In the case of the minimal Z' models, limits are set on the effective couplings as a function of the resonance mass to incorporate interference effects of the Z' signal with the Drell-Yan background.

A. Limits on narrow spin-1 Z'_{SSM}, E_6 Z', and Z^* bosons

For the Z'_{SSM}, E_6-motivated Z' and Z^* bosons, the model specifies the boson's coupling strength to SM fermions and therefore the intrinsic width. The parameter of interest in the likelihood analysis is therefore σB as a function of the new boson's mass.

TABLE VI. Values of σB for the different models. The model parameter M corresponds to the mass of the Z', Z'_χ, Z'_ψ, Z^*, and G^* boson. For the QBH models, $M = M_{\mathrm{th}}$ corresponds to the threshold mass, while for the MWT model $M = M_{R_1}$. The value $M = 3$ TeV is not applicable for the MWT model, as the range of the limits is up to 2.25 TeV.

	σB [fb]		
Model	$M = 1$ TeV	$M = 2$ TeV	$M = 3$ TeV
Z'_{SSM}	170	3.4	0.21
Z'_χ	93	1.5	0.062
Z'_ψ	47	0.87	0.032
Z^*	300	4.0	0.076
G^*, $k/\bar{M}_{\mathrm{Pl}} = 0.1$	190	1.8	0.044
RS QBH	56	0.40	0.0065
ADD QBH	11000	96	1.8
MWT, $\tilde{g} = 2$	31	0.17	N/A

Figure 3 presents the expected and observed exclusion limits on σB at 95% C.L. for the combined dielectron and dimuon channels for the Z'_{SSM} search. The observed limit is within the $\pm 2\sigma$ band of expected limits for all $M_{Z'}$. Figure 3 also contains the Z'_{SSM} theory band for σB. Its width represents the theoretical uncertainty, taking into account the following sources: the PDF error set, the choice of PDF, and α_S. The value of $M_{Z'}$ at which the theory curve and the observed (expected) 95% C.L. limits on σB intersect is interpreted as the observed (expected) mass limit for the Z'_{SSM} boson, and corresponds to 2.90 (2.87) TeV.

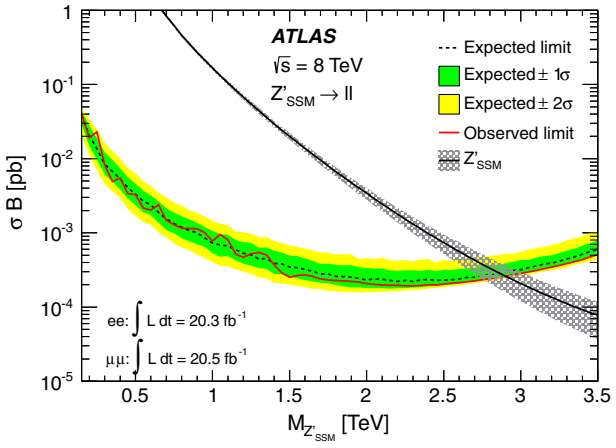

FIG. 3 (color online). Median expected (dashed line) and observed (solid red line) 95% C.L. upper limits on cross section times branching ratio (σB) in the combined dilepton channel, along with predicted σB for Z'_{SSM} production. The inner and outer bands show the range in which the limit is expected to lie in 68% and 95% of pseudoexperiments, respectively. The thickness of the Z'_{SSM} theory curve represents the theoretical uncertainty from the PDF error set and α_S, as well as the choice of PDF.

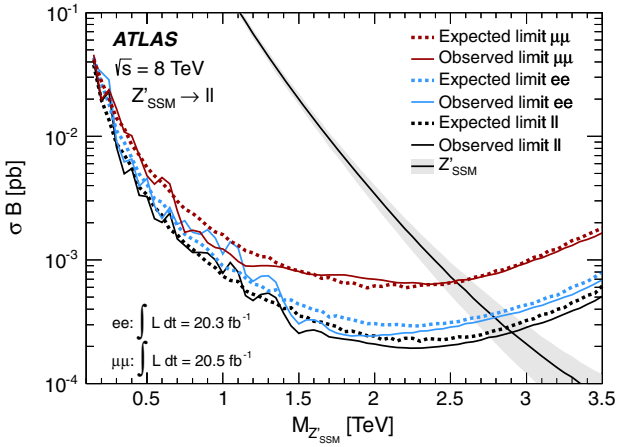

FIG. 4 (color online). Median expected (dashed line) and observed (solid line) 95% C.L. upper limits on cross section times branching ratio (σB) for Z'_{SSM} production for the exclusive dimuon and dielectron channels, and for both channels combined. The width of the Z'_{SSM} theory band represents the theoretical uncertainty from the PDF error set, the choice of PDF, as well as α_S.

A comparison of the combined limits on σB and those for the exclusive dielectron and dimuon channel is given in Fig. 4. This demonstrates the contribution of each channel to the combined limit. As expected from Fig. 1, the larger values for $A \times \epsilon$ in addition to the better resolution in the dielectron channel results in a stronger limit than in the dimuon channel. The observed (expected) Z'_{SSM} mass limit is 2.79 (2.76) TeV in the dielectron channel, and 2.53 (2.53) TeV in the dimuon channel.

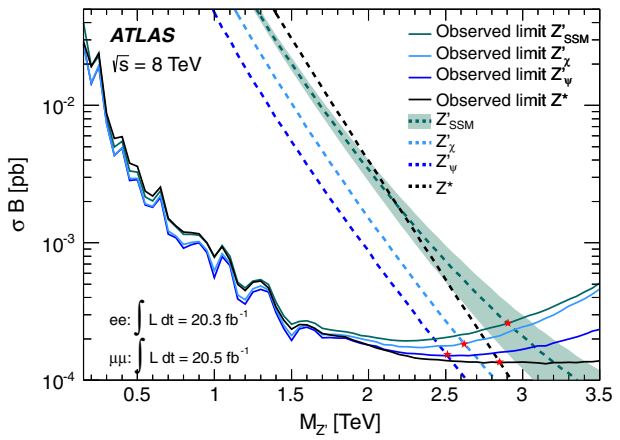

FIG. 5 (color online). Observed upper cross section times branching ratio (σB) limits at 95% C.L. for Z'_{SSM}, E_6-motivated Z' and Z^* bosons using the combined dilepton channel. In addition, theoretical cross sections on σB are shown for the same models. The stars indicate the lower mass limits for each considered model. The width of the Z'_{SSM} band represents the theoretical uncertainty from the PDF error set, the choice of PDF, as well as α_S. The width of the Z'_{SSM} band applies to the E_6-motivated Z' curves as well.

TABLE VII. Observed and expected lower mass limits for Z' and Z^* bosons, using the corresponding signal template for a given model.

Model	Width [%]	Observed limit [TeV]	Expected limit [TeV]
Z'_{SSM}	3.0	2.90	2.87
Z'_{χ}	1.2	2.62	2.60
Z'_{ψ}	0.5	2.51	2.46
Z^*	3.4	2.85	2.82

Figure 5 shows the observed σB exclusion limits at 95% C.L. for the Z'_{SSM}, Z'_{χ}, Z'_{ψ}, and Z^* signal searches. Here only observed limits are shown, as they are always very similar to the expected limits (see Fig. 4). The theoretical σB of the boson for the Z'_{SSM}, two E_6-motivated models, and Z^* are also displayed. The 95% C.L. limits on σB are used to set mass limits for each of the considered models. Mass limits obtained for the Z'_{SSM}, E_6-motivated Z' and Z^* bosons are displayed in Table VII.

As demonstrated in Fig. 5, for lower values of $M_{Z'}$ the limit is driven primarily by the width of the signal and gets stronger with decreasing width. At large $M_{Z'}$, the σB limit for a given Z' model worsens with increasing mass. This weakening of the limit is due to the presence of the parton-luminosity tail in the $m_{\ell\ell}$ line shape. The magnitude of this degradation is proportional to the size of the low-mass tail of the signal due to much higher background levels at low $m_{\ell\ell}$ compared to high $m_{\ell\ell}$. All Z' models exhibit a parton-luminosity tail, the size of which increases with increasing natural width of the Z' resonance. The tail is most pronounced for Z'_{SSM}, and least for Z'_{ψ}, in line with the different widths given in Table VII. Even though the width of the Z^* is similar to the width of the Z'_{SSM}, the tensor form of the coupling of the Z^* to fermions strongly suppresses parton-luminosity effects. Limits on σB for the Z^* interpretation therefore do not worsen with increasing invariant mass. Quantitatively, the observed Z'_{SSM} mass limit would increase from 2.90 to 2.95 TeV and 3.08 TeV, if the Z'_{χ} and Z'_{ψ} boson signal templates, with smaller widths, were used. If the Z^* boson template with negligible parton-luminosity tail but similar width were used instead of the Z'_{SSM} template, the observed limit would increase to 3.20 TeV.

B. Limits on minimal Z' bosons

Limits are also set in the minimal Z' models parametrization [4] of the Z' boson couplings introduced in Sec. II B. Instead of using the predicted σB based on a fixed coupling to fermions as described in the previous section, the new boson is characterized by two coupling parameters, $g_{\mathrm{B\text{-}L}}$ and g_{Y}.

For this analysis, the signal templates account for the dependence of the Z' boson width on γ' and θ_{min}, as well as the interference with SM Z/γ^*. For a given value of θ_{min}

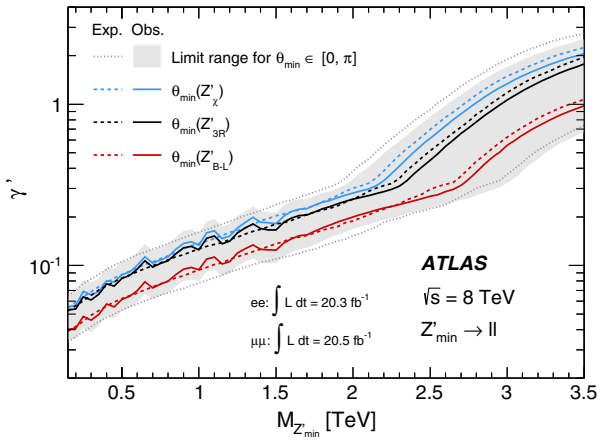

FIG. 6 (color online). Expected (dotted and dashed lines) and observed (filled area and lines) limits at 95% C.L. on the strength of the Z' boson coupling relative to that of the SM Z boson (γ') for the combined dielectron and dimuon channels as a function of the Z'_{min} mass in the minimal Z' models parametrization. Limit curves are shown for three representative values of the mixing between the generators of the B-L and the weak hypercharge Y gauge groups (θ_{min}). These are $\tan\theta_{\mathrm{min}} = 0$, $\tan\theta_{\mathrm{min}} = -2$, and $\tan\theta_{\mathrm{min}} = -0.8$, which correspond respectively to the $Z'_{\mathrm{B\text{-}L}}$, $Z'_{3\mathrm{R}}$, and Z'_{χ} models at specific values of γ'. The region above each line is excluded. The gray band envelops all observed limit curves, which depend on the choice of $\theta_{\mathrm{min}} \in [0, \pi]$. The corresponding expected limit curves are within the area delimited by the two dotted lines.

and for each tested Z' mass, dilepton invariant mass templates are created with various γ' values between 0.005 and 4. The templates at these chosen values of γ' are interpolated to other values of γ' by using a smooth

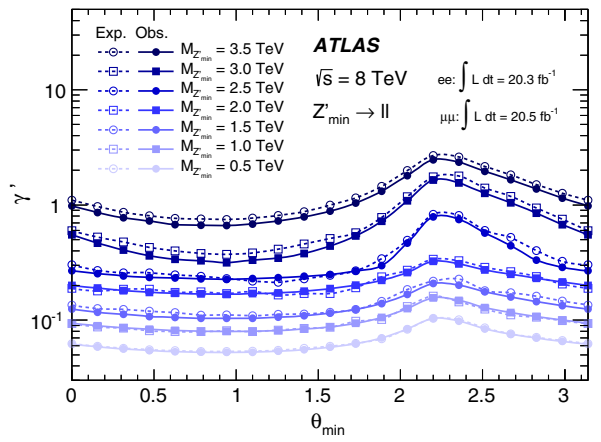

FIG. 7 (color online). Expected (empty markers and dashed lines) and observed (filled markers and lines) limits at 95% C.L. on the strength of the Z' boson coupling relative to that of the SM Z boson (γ') for the combined dielectron and dimuon channels as a function of the mixing between the generators of the B-L and the weak hypercharge Y gauge groups (θ_{min}) in the minimal Z' models parametrization. The limits are set for several representative values of the mass of the Z' boson, $M_{Z'_{\mathrm{min}}}$. The region above each line is excluded.

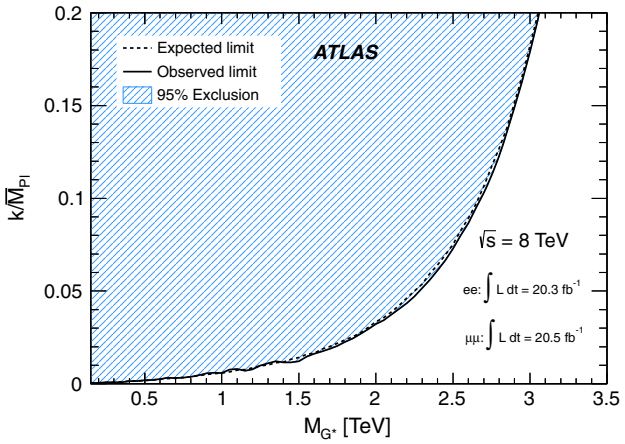

FIG. 8 (color online). Expected and observed 95% C.L. limits in the plane of the coupling strength of the Randall-Sundrum G^* to SM particles ($k/\bar{M}_{\mathrm{Pl}}$) versus G^* mass for the combination of the dielectron and dimuon channels. The region above the curve is excluded at 95% C.L.

interpolating function in each dilepton mass bin. The parameter of interest in the likelihood analysis is γ' for specific values of θ_{min} and the Z' boson mass, $M_{Z'_{\mathrm{min}}}$. Systematic uncertainties are included in the analysis analogously to the computation of σB limits described above. Limits at 95% C.L. are set on the relative coupling strength γ' as a function of the Z'_{min} boson mass, as shown in Fig. 6. Figure 7 contains limits at 95% C.L. on γ' versus θ_{min} for several representative values of $M_{Z'_{\mathrm{min}}}$. The strongest and weakest limits are found for $\theta_{\mathrm{min}} = 0.96$ and $\theta_{\mathrm{min}} = 2.27$, respectively. The limits depend heavily on the Z' branching ratio to dileptons, which in turn depends on θ_{min} as the choice of this parameter influences the Z' couplings. For $M_{Z'_{\mathrm{min}}}$ significantly above the $t\bar{t}$ production threshold, the sum of Z' branching ratios to electron and muon pairs ranges from 4.6% to 32%.

C. Limits on spin-2 graviton excitations in Randall-Sundrum models

The phenomenology of RS models is characterized by the G^* mass and $k/\bar{M}_{\mathrm{Pl}}$. Limits at 95% C.L. on $\sigma B(G^* \to \ell^+\ell^-)$ are obtained and compared to the theoretical σB assuming values of $k/\bar{M}_{\mathrm{Pl}}$ less than 0.2. These results are used to set limits in the plane of $k/\bar{M}_{\mathrm{Pl}}$ versus G^* mass, as illustrated in Fig. 8 for the combined dilepton channel.

TABLE VIII. Observed and expected 95% C.L. lower limits on the mass of the G^* with varying coupling $k/\bar{M}_{\mathrm{Pl}}$. The two lepton channels are combined.

$k/\bar{M}_{\mathrm{Pl}}$	0.01	0.03	0.05	0.1	0.2
Observed limit on M_{G^*} [TeV]	1.25	1.96	2.28	2.68	3.05
Expected limit on M_{G^*} [TeV]	1.28	1.95	2.25	2.67	3.05

Mass limits for five of the $k/\bar{M}_{\rm Pl}$ values used are given in Table VIII.

D. Limits on quantum black hole models

Upper limits at 95% C.L. on σB are set as a function of $M_{\rm th}$, assuming a signal according to both the RS and ADD models. While the two models predict different mass distributions, using the same σB limit curve for each (as in Fig. 9) affects the mass limits obtained by only 1%. The observed lower limits on $M_{\rm th}$ for the combination of the two dilepton channels are 3.65 TeV for the ADD model and 2.24 TeV for the RS model.

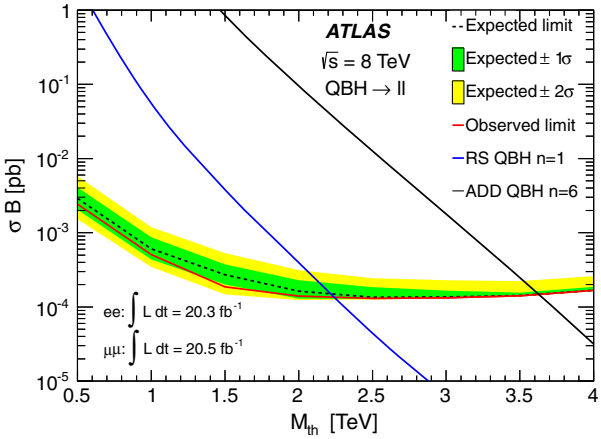

FIG. 9 (color online). Expected and observed 95% C.L. upper limits on cross section times branching ratio (σB) for quantum black hole production in the extra-dimensional model proposed by ADD and RS for the combined dilepton channel.

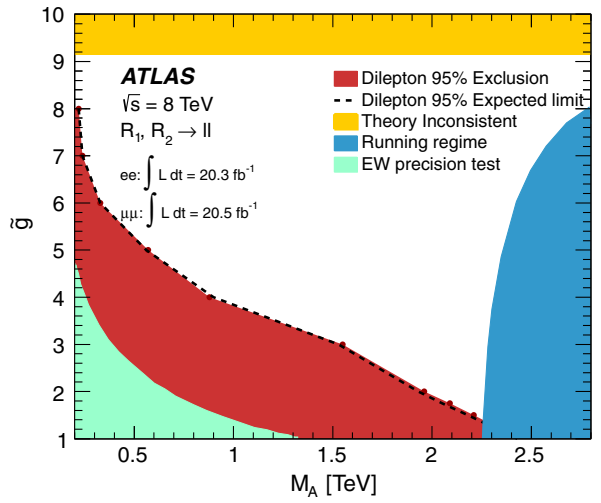

FIG. 10 (color online). Exclusion contours at 95% C.L. in the plane of the minimal walking technicolor parameter space defined by the bare axial-vector mass versus the strength of the spin-1 resonance interaction (M_A, $\tilde{g}$). Electroweak precision measurements exclude the green area in the bottom left corner. The requirement to stay in the walking regime excludes the blue area in the right corner. The red area (black dashed line) shows the observed (expected) exclusion for both channels combined. The upper region is excluded due to nonreal axial and axial-vector decay constants.

TABLE IX. Combined 95% C.L. observed and expected lower mass limits on M_{R_1} and M_A (minimal walking technicolor model) for various values of $\tilde{g}$.

$\tilde{g}$	1.5	2	3	4	5	6	7	8
Observed limit M_{R_1} [TeV]	2.27	1.99	1.57	0.89	0.57	0.33	0.24	0.22
Expected limit M_{R_1} [TeV]	2.24	1.96	1.54	0.90	0.56	0.33	0.24	0.22
Observed limit M_A [TeV]	2.21	1.96	1.55	0.88	0.57	0.33	0.24	0.22
Expected limit M_A [TeV]	2.18	1.93	1.53	0.90	0.56	0.33	0.24	0.22

E. Limits on minimal walking technicolor

The MWT model introduced in Sec. II F is tested by searching for technimeson resonances. Limits on σB are set at 95% C.L. as a function of M_{R_1} for $\tilde{g} = 2$. Electroweak precision data, a requirement to stay in the walking technicolor regime and constraints from requiring real-valued physical decay constants exclude a portion of the $\tilde{g}$ versus M_A plane, as shown in Fig. 10. By combining these factors and the 95% C.L. limits that are set, all possible M_A masses are excluded for $\tilde{g}$ less than ≈1.4. Limits on M_{R_1} for various values of $\tilde{g}$ are given in Table IX.

XIII. CONCLUSIONS

In conclusion, the ATLAS detector at the Large Hadron Collider was used to search for resonances decaying to dielectron or dimuon final states at masses above the pole mass of the Z boson, using 20.3 fb^{-1} of proton-proton collision data collected in 2012 at $\sqrt{s} = 8$ TeV in the dielectron channel, and 20.5 fb^{-1} in the dimuon channel. The observed invariant mass spectrum is consistent with the Standard Model expectation. Limits are set on signal cross section times branching fraction for a variety of physics scenarios beyond the Standard Model. For the benchmark $Z'_{\rm SSM}$ boson with a mass of 2.5 TeV, the expected cross-section limit improved approximately fivefold in comparison to the previous ATLAS publication, which used $\sqrt{s} =$ 7 TeV data collected in 2011. The limit on the mass of the benchmark $Z'_{\rm SSM}$ signal improved from 2.22 to 2.90 TeV, and mass limits of 2.51–2.62 TeV are set for various E_6-motivated Z' bosons. For Z^* bosons, the mass limit is 2.85 TeV, and the limit on the mass of the G^* in the Randall-Sundrum model with coupling parameter $k/\bar{M}_{\rm Pl}$

equal to 0.1 is 2.68 TeV. Experimental limits are also set on minimal Z' models and on a minimal walking technicolor model with a composite Higgs boson. The limits set on the production threshold of quantum black holes are 3.65 TeV for the extra-dimensional model proposed by Arkani-Hamed, Dimopoulos, and Dvali and 2.24 TeV for the Randall-Sundrum model. For all but those on quantum black hole production, the limits presented are the most stringent to date.

ACKNOWLEDGMENTS

We thank T. Hapola for implementing the minimal walking technicolor model using MADGRAPH to generate the signal and for his help with acceptance studies. The limits shown in Sec. XII were calculated using computing resources provided by the Argonne Leadership Computing Facility and the National Energy Research Scientific Computing Center. We thank CERN for the very successful operation of the LHC, as well as the support staff from our institutions without whom ATLAS could not be operated efficiently. We acknowledge the support of ANPCyT, Argentina; YerPhI, Armenia; ARC, Australia; BMWF and FWF, Austria; ANAS, Azerbaijan; SSTC, Belarus; CNPq and FAPESP, Brazil; NSERC, NRC, and CFI, Canada; CERN; CONICYT, Chile; CAS, MOST, and NSFC, China; COLCIENCIAS, Colombia; MSMT CR, MPO CR, and VSC CR, Czech Republic; DNRF, DNSRC, and Lundbeck Foundation, Denmark; EPLANET, ERC, and NSRF, European Union; IN2P3-CNRS, CEA-DSM/IRFU, France; GNSF, Georgia; BMBF, DFG, HGF, MPG, and AvH Foundation, Germany; GSRT and NSRF, Greece; ISF, MINERVA, GIF, I-CORE, and Benoziyo Center, Israel; INFN, Italy; MEXT and JSPS, Japan; CNRST, Morocco; FOM and NWO, Netherlands; BRF and RCN, Norway; MNiSW and NCN, Poland; GRICES and FCT, Portugal; MNE/IFA, Romania; MES of Russia and ROSATOM, Russian Federation; JINR, MSTD, Serbia; MSSR, Slovakia; ARRS and MIZŠ, Slovenia; DST/NRF, South Africa; MINECO, Spain; SRC and Wallenberg Foundation, Sweden; SER, SNSF, and Cantons of Bern and Geneva, Switzerland; NSC, Taiwan; TAEK, Turkey; STFC, the Royal Society and Leverhulme Trust, United Kingdom; DOE and NSF, United States of America. The crucial computing support from all WLCG partners is acknowledged gratefully, in particular from CERN and the ATLAS Tier-1 facilities at TRIUMF (Canada), NDGF (Denmark, Norway, Sweden), CC-IN2P3 (France), KIT/GridKA (Germany), INFN-CNAF (Italy), NL-T1 (Netherlands), PIC (Spain), ASGC (Taiwan), RAL (UK), and BNL (USA) and in the Tier-2 facilities worldwide.

[1] ATLAS Collaboration, JINST **3**, S08003 (2008).
[2] D. London and J. L. Rosner, Phys. Rev. D **34**, 1530 (1986).
[3] P. Langacker, Rev. Mod. Phys. **81**, 1199 (2009).
[4] E. Salvioni, G. Villadoro, and F. Zwirner, J. High Energy Phys. 11 (2009) 068.
[5] ATLAS Collaboration, Phys. Lett. B **716**, 1 (2012).
[6] CMS Collaboration, Phys. Lett. B **716**, 30 (2012).
[7] M. V. Chizhov, V. A. Bednyakov, and J. A. Budagov, Phys. At. Nucl. **71**, 2096 (2008).
[8] M. V. Chizhov and G. Dvali, Phys. Lett. B **703**, 593 (2011).
[9] M. V. Chizhov, Phys. Part. Nucl. Lett. **8**, 512 (2011).
[10] M. V. Chizhov, V. A. Bednyakov, and J. A. Budagov, Nuovo Cimento Soc. Ital. Fis. **33C**, 343 (2010).
[11] L. Randall and R. Sundrum, Phys. Rev. Lett. **83**, 3370 (1999).
[12] P. Meade and L. Randall, J. High Energy Phys. 05 (2008) 003.
[13] F. Sannino and K. Tuominen, Phys. Rev. D **71**, 051901 (2005).
[14] D. D. Dietrich, F. Sannino, and K. Tuominen, Phys. Rev. D **72**, 055001 (2005).
[15] R. Foadi, M. T. Frandsen, T. A. Ryttov, and F. Sannino, Phys. Rev. D **76**, 055005 (2007).
[16] R. Foadi, M. T. Frandsen, and F. Sannino, Phys. Rev. D **87**, 095001 (2013).
[17] ATLAS Collaboration, J. High Energy Phys. 11 (2012) 138.
[18] CMS Collaboration, Phys. Lett. B **720**, 63 (2013).
[19] V. M. Abazov *et al.* (D0 Collaboration), Phys. Lett. B **695**, 88 (2011).
[20] T. Aaltonen *et al.* (CDF Collaboration), Phys. Rev. Lett. **106**, 121801 (2011).
[21] G. Abbiendi *et al.* (The OPAL Collaboration), Eur. Phys. J. C **33**, 173 (2004).
[22] J. Abdallah (DELPHI Collaboration), Eur. Phys. J. C **45**, 589 (2006).
[23] P. Achard *et al.* (L3 Collaboration), Eur. Phys. J. C **47**, 1 (2006).
[24] S. Schael *et al.* (ALEPH Collaboration), Eur. Phys. J. C **49**, 411 (2007).
[25] P. Langacker, arXiv:0911.4294.
[26] M. Dittmar, A.-S. Nicollerat, and A. Djouadi, Phys. Lett. B **583**, 111 (2004).
[27] E. Accomando, A. Belyaev, L. Fedeli, S. F. King, and C. Shepherd-Themistocleous, Phys. Rev. D **83**, 075012 (2011).
[28] G. Senjanovic and R. N. Mohapatra, Phys. Rev. D **12**, 1502 (1975).
[29] R. N. Mohapatra and J. C. Pati, Phys. Rev. D **11**, 566 (1975).
[30] L. Basso, A. Belyaev, S. Moretti, and C. H. Shepherd-Themistocleous, Phys. Rev. D **80**, 055030 (2009).
[31] H. Davoudiasl, J. L. Hewett, and T. G. Rizzo, Phys. Rev. Lett. **84**, 2080 (2000).
[32] D. Dimopoulos and G. Landsberg, Phys. Rev. Lett. **87**, 161602 (2001).

[33] S. B. Giddings and S. Thomas, Phys. Rev. D **65**, 056010 (2002).
[34] D. M. Gingrich and K. Martell, Phys. Rev. D **78**, 115009 (2008).
[35] X. Calmet, W. Gong, and S. D. H. Hsu, Phys. Lett. B **668**, 20 (2008).
[36] N. Arkani-Hamed, S. Dimopoulos, and G. Dvali, Phys. Lett. B **429**, 263 (1998).
[37] D. M. Gingrich, J. Phys. G **37**, 105008 (2010).
[38] ATLAS Collaboration, Phys. Lett. B **728**, 562 (2014).
[39] ATLAS Collaboration, Phys. Rev. Lett. **112**, 091804 (2014).
[40] CMS Collaboration, J. High Energy Phys. 07 (2013) 178.
[41] D.-C. Dai, G. Starkman, D. Stojkovic, C. Issever, E. Rizvi, and J. Tseng, Phys. Rev. D **77**, 076007 (2008).
[42] ATLAS Collaboration, J. High Energy Phys. 01 (2013) 029.
[43] J. R. Andersen, T. Hapola, and F. Sannino, Phys. Rev. D **85**, 055017 (2012).
[44] A. Belyaev, R. Foadi, M. T. Frandsen, M. Järvinen, F. Sannino, and A. Pukhov, Phys. Rev. D **79**, 035006 (2009).
[45] ATLAS Collaboration, Eur. Phys. J. C **72**, 1849 (2012).
[46] ATLAS Collaboration, Eur. Phys. J. C **74**, 2941 (2014).
[47] S. Alioli, P. Nason, C. Oleari, and E. Re, J. High Energy Phys. 06 (2010) 043.
[48] H.-L. Lai, M. Guzzi, J. Huston, Z. Li, P. M. Nadolsky, J. Pumplin, and C.-P. Yuan, Phys. Rev. D **82**, 074024 (2010).
[49] T. Sjöstrand, S. Mrenna, and P. Z. Skands, Comput. Phys. Commun. **178**, 852 (2008).
[50] P. Golonka and Z. Wąs, Eur. Phys. J. C **45**, 97 (2006).
[51] ATLAS Collaboration, Eur. Phys. J. C **70**, 823 (2010).
[52] S. Agostinelli *et al.* (GEANT4 Collaboration), Nucl. Instrum. Methods Phys. Res., Sect. A **506**, 250 (2003).
[53] K. Melnikov and F. Petriello, Phys. Rev. D **74**, 114017 (2006).
[54] Y. Li and F. Petriello, Phys. Rev. D **86**, 094034 (2012).
[55] A. D. Martin, W. J. Stirling, R. S. Thorne, and G. Watt, Eur. Phys. J. C **63**, 189 (2009).
[56] A. D. Martin, R. G. Roberts, W. J. Stirling, and R. S. Thorne, Eur. Phys. J. C **39**, 155 (2005).
[57] D. Bardin, S. Bondarenko, P. Christova, L. Kalinovskaya, L. Rumyantsev, A. Sapronov, and W. von Schlippe, JETP Lett. **96**, 285 (2012).
[58] S. G. Bondarenko and A. A. Sapronov, Comput. Phys. Commun. **184**, 2343 (2013).
[59] J. Alwall, M. Herquet, F. Maltoni, O. Mattelaer, and T. Stelzer, J. High Energy Phys. 06 (2011) 128.
[60] U. Baur, Phys. Rev. D **75**, 013005 (2007).
[61] G. Corcella, I. G. Knowles, G. Marchesini, S. Moretti, K. Odagiri, P. Richardson, M. H. Seymour, and B. R. Webber, J. High Energy Phys. 01 (2001) 010.
[62] G. Corcella *et al.*, arXiv:hep-ph/0210213.
[63] J. Pumplin, D. R. Stump, J. Huston, H.-L. Lai, P. Nadolsky, and W.-K. Tung, J. High Energy Phys. 07 (2002) 012.
[64] J. M. Campbell and R. K. Ellis, Phys. Rev. D **60**, 113006 (1999).
[65] S. Frixione and B. R. Webber, J. High Energy Phys. 06 (2002) 029.
[66] S. Frixione, P. Nason, and B. R. Webber, J. High Energy Phys. 08 (2003) 007.
[67] S. Frixione, E. Laenen, P. Motylinski, C. White, and B. R. Webber, J. High Energy Phys. 07 (2008) 029.
[68] M. Cacciari, M. Czakon, M. Mangano, A. Mitov, and P. Nason, Phys. Lett. B **710**, 612 (2012).
[69] P. Bärnreuther, M. Czakon, and A. Mitov, Phys. Rev. Lett. **109**, 132001 (2012).
[70] M. Czakon and A. Mitov, J. High Energy Phys. 12 (2012) 054.
[71] M. Czakon and A. Mitov, J. High Energy Phys. 01 (2013) 080.
[72] M. Czakon, P. Fiedler, and A. Mitov, Phys. Rev. Lett. **110**, 252004 (2013).
[73] M. Czakon and A. Mitov, arXiv:1112.5675.
[74] M. Botje *et al.*, arXiv:1101.0538.
[75] A. D. Martin, W. J. Stirling, R. S. Thorne, and G. Watt, Eur. Phys. J. C **64**, 653 (2009).
[76] J. Gao, M. Guzzi, J. Huston, H.-L. Lai, Z. Li, P. Nadolsky, J. Pumplin, D. Stump, and C.-P. Yuan, Phys. Rev. D **89**, 033009 (2014).
[77] R. Ball *et al.*, Nucl. Phys. **B867**, 244 (2013).
[78] N. Kidonakis, Phys. Rev. D **82**, 054018 (2010).
[79] A. Belyaev, N. D. Christensen, and A. Pukhov, Comput. Phys. Commun. **184**, 1729 (2013).
[80] D. M. Gingrich, Comput. Phys. Commun. **181**, 1917 (2010), http://qbh.hepforge.org/.
[81] P. Mathews, V. Ravindran, K. Sridhar, and W. L. van Neerven, Nucl. Phys. **B713**, 333 (2005).
[82] P. Mathews, V. Ravindran, and K. Sridhar, J. High Energy Phys. 10 (2005) 031.
[83] M. C. Kumar, P. Mathews, and V. Ravindran, Eur. Phys. J. C **49**, 599 (2007).
[84] ATLAS Collaboration, Eur. Phys. J. C **72**, 1909 (2012).
[85] ATLAS Collaboration, arXiv:1404.4562.
[86] ATLAS Collaboration, Report No. ATLAS-CONF-2013-088, 2013, http://cds.cern.ch/record/1580207.
[87] ATLAS Collaboration, Phys. Rev. Lett. **107**, 272002 (2011).
[88] C. Anastasiou, L. Dixon, K. Melnikov, and F. Petriello, Phys. Rev. D **69**, 094008 (2004).
[89] S. Alekhin, J. Blumlein, and S. Moch, Phys. Rev. D **86**, 054009 (2012).
[90] F. D. Aaron *et al.* (H1 and ZEUS Collaborations), J. High Energy Phys. 01 (2010) 109.
[91] J. Wenninger, Report No. CERN-ATS-2013-040, 2013, http://cds.cern.ch/record/1546734.
[92] ATLAS Collaboration, Phys. Lett. B **700**, 163 (2011).
[93] T. Aaltonen *et al.* (CDF Collaboration), Phys. Rev. Lett. **102**, 091805 (2009).
[94] A. Caldwell, D. Kollar, and K. Kröninger, Comput. Phys. Commun. **180**, 2197 (2009).

G. Aad,[84] B. Abbott,[112] J. Abdallah,[152] S. Abdel Khalek,[116] O. Abdinov,[11] R. Aben,[106] B. Abi,[113] M. Abolins,[89] O. S. AbouZeid,[159] H. Abramowicz,[154] H. Abreu,[153] R. Abreu,[30] Y. Abulaiti,[147a,147b] B. S. Acharya,[165a,165b,b] L. Adamczyk,[38a] D. L. Adams,[25] J. Adelman,[177] S. Adomeit,[99] T. Adye,[130] T. Agatonovic-Jovin,[13a] J. A. Aguilar-Saavedra,[125f,125a] M. Agustoni,[17] S. P. Ahlen,[22] F. Ahmadov,[64,c] G. Aielli,[134a,134b] H. Akerstedt,[147a,147b] T. P. A. Åkesson,[80] G. Akimoto,[156] A. V. Akimov,[95] G. L. Alberghi,[20a,20b] J. Albert,[170] S. Albrand,[55] M. J. Alconada Verzini,[70] M. Aleksa,[30] I. N. Aleksandrov,[64] C. Alexa,[26a] G. Alexander,[154] G. Alexandre,[49] T. Alexopoulos,[10] M. Alhroob,[165a,165c] G. Alimonti,[90a] L. Alio,[84] J. Alison,[31] B. M. M. Allbrooke,[18] K. Allen,[160a,d] L. J. Allison,[71] P. P. Allport,[73] J. Almond,[83] A. Aloisio,[103a,103b] A. Alonso,[36] F. Alonso,[70] C. Alpigiani,[75] A. Altheimer,[35] B. Alvarez Gonzalez,[89] M. G. Alviggi,[103a,103b] K. Amako,[65] Y. Amaral Coutinho,[24a] C. Amelung,[23] D. Amidei,[88] S. P. Amor Dos Santos,[125a,125c] A. Amorim,[125a,125b] S. Amoroso,[48] N. Amram,[154] G. Amundsen,[23] C. Anastopoulos,[140] L. S. Ancu,[49] N. Andari,[30] T. Andeen,[35] C. F. Anders,[58b] G. Anders,[30] K. J. Anderson,[31] A. Andreazza,[90a,90b] V. Andrei,[58a] X. S. Anduaga,[70] S. Angelidakis,[9] I. Angelozzi,[106] P. Anger,[44] A. Angerami,[35] F. Anghinolfi,[30] A. V. Anisenkov,[108] N. Anjos,[125a] A. Annovi,[47] A. Antonaki,[9] M. Antonelli,[47] A. Antonov,[97] J. Antos,[145b] F. Anulli,[133a] M. Aoki,[65] L. Aperio Bella,[18] R. Apolle,[119,e] G. Arabidze,[89] I. Aracena,[144] Y. Arai,[65] J. P. Araque,[125a] A. T. H. Arce,[45] J-F. Arguin,[94] S. Argyropoulos,[42] M. Arik,[19a] A. J. Armbruster,[30] O. Arnaez,[30] V. Arnal,[81] H. Arnold,[48] M. Arratia,[28] O. Arslan,[21] A. Artamonov,[96] G. Artoni,[23] S. Asai,[156] N. Asbah,[42] A. Ashkenazi,[154] B. Åsman,[147a,147b] L. Asquith,[6] K. Assamagan,[25] R. Astalos,[145a] M. Atkinson,[166] N. B. Atlay,[142] B. Auerbach,[6] K. Augsten,[127] M. Aurousseau,[146b] G. Avolio,[30] G. Azuelos,[94,f] Y. Azuma,[156] M. A. Baak,[30] C. Bacci,[135a,135b] H. Bachacou,[137] K. Bachas,[155] M. Backes,[30] M. Backhaus,[30] J. Backus Mayes,[144] E. Badescu,[26a] P. Bagiacchi,[133a,133b] P. Bagnaia,[133a,133b] Y. Bai,[33a] T. Bain,[35] J. T. Baines,[130] O. K. Baker,[177] S. Baker,[77] P. Balek,[128] F. Balli,[137] E. Banas,[39] Sw. Banerjee,[174] A. A. E. Bannoura,[176] V. Bansal,[170] H. S. Bansil,[18] L. Barak,[173] S. P. Baranov,[95] E. L. Barberio,[87] D. Barberis,[50a,50b] M. Barbero,[84] T. Barillari,[100] M. Barisonzi,[176] T. Barklow,[144] N. Barlow,[28] B. M. Barnett,[130] R. M. Barnett,[15] Z. Barnovska,[5] A. Baroncelli,[135a] G. Barone,[49] A. J. Barr,[119] F. Barreiro,[81] J. Barreiro Guimarães da Costa,[57] R. Bartoldus,[144] A. E. Barton,[71] P. Bartos,[145a] V. Bartsch,[150] A. Bassalat,[116] A. Basye,[166] R. L. Bates,[53] L. Batkova,[145a] J. R. Batley,[28] M. Battaglia,[138] M. Battistin,[30] F. Bauer,[137] H. S. Bawa,[144,g] T. Beau,[79] P. H. Beauchemin,[162] R. Beccherle,[123a,123b] P. Bechtle,[21] H. P. Beck,[17] K. Becker,[176] S. Becker,[99] M. Beckingham,[139] C. Becot,[116] A. J. Beddall,[19c] A. Beddall,[19c] S. Bedikian,[177] V. A. Bednyakov,[64] C. P. Bee,[149] L. J. Beemster,[106] T. A. Beermann,[176] M. Begel,[25] K. Behr,[119] C. Belanger-Champagne,[86] P. J. Bell,[49] W. H. Bell,[49] G. Bella,[154] L. Bellagamba,[20a] A. Bellerive,[29] M. Bellomo,[85] K. Belotskiy,[97] O. Beltramello,[30] O. Benary,[154] D. Benchekroun,[136a] K. Bendtz,[147a,147b] N. Benekos,[166] Y. Benhammou,[154] E. Benhar Noccioli,[49] J. A. Benitez Garcia,[160b] D. P. Benjamin,[45] J. R. Bensinger,[23] K. Benslama,[131] S. Bentvelsen,[106] D. Berge,[106] E. Bergeaas Kuutmann,[16] N. Berger,[5] F. Berghaus,[170] E. Berglund,[106] J. Beringer,[15] C. Bernard,[22] P. Bernat,[77] C. Bernius,[78] F. U. Bernlochner,[170] T. Berry,[76] P. Berta,[128] C. Bertella,[84] G. Bertoli,[147a,147b] F. Bertolucci,[123a,123b] D. Bertsche,[112] M. I. Besana,[90a] G. J. Besjes,[105] O. Bessidskaia,[147a,147b] M. F. Bessner,[42] N. Besson,[137] C. Betancourt,[48] S. Bethke,[100] W. Bhimji,[46] R. M. Bianchi,[124] L. Bianchini,[23] M. Bianco,[30] O. Biebel,[99] S. P. Bieniek,[77] K. Bierwagen,[54] J. Biesiada,[15] M. Biglietti,[135a] J. Bilbao De Mendizabal,[49] H. Bilokon,[47] M. Bindi,[54] S. Binet,[116] A. Bingul,[19c] C. Bini,[133a,133b] C. W. Black,[151] J. E. Black,[144] K. M. Black,[22] D. Blackburn,[139] R. E. Blair,[6] J.-B. Blanchard,[137] T. Blazek,[145a] I. Bloch,[42] C. Blocker,[23] W. Blum,[82,a] U. Blumenschein,[54] G. J. Bobbink,[106] V. S. Bobrovnikov,[108] S. S. Bocchetta,[80] A. Bocci,[45] C. Bock,[99] C. R. Boddy,[119] M. Boehler,[48] J. Boek,[176] T. T. Boek,[176] J. A. Bogaerts,[30] A. G. Bogdanchikov,[108] A. Bogouch,[91,a] C. Bohm,[147a] J. Bohm,[126] V. Boisvert,[76] T. Bold,[38a] V. Boldea,[26a] A. S. Boldyrev,[98] M. Bomben,[79] M. Bona,[75] M. Boonekamp,[137] A. Borisov,[129] G. Borissov,[71] M. Borri,[83] S. Borroni,[42] J. Bortfeldt,[99] V. Bortolotto,[135a,135b] K. Bos,[106] D. Boscherini,[20a] M. Bosman,[12] H. Boterenbrood,[106] J. Boudreau,[124] J. Bouffard,[2] E. V. Bouhova-Thacker,[71] D. Boumediene,[34] C. Bourdarios,[116] N. Bousson,[113] S. Boutouil,[136d] A. Boveia,[31] J. Boyd,[30] I. R. Boyko,[64] I. Bozovic-Jelisavcic,[13b] J. Bracinik,[18] A. Brandt,[8] G. Brandt,[15] O. Brandt,[58a] U. Bratzler,[157] B. Brau,[85] J. E. Brau,[115] H. M. Braun,[176,a] S. F. Brazzale,[165a,165c] B. Brelier,[159] K. Brendlinger,[121] A. J. Brennan,[87] R. Brenner,[167] S. Bressler,[173] K. Bristow,[146c] T. M. Bristow,[46] D. Britton,[53] F. M. Brochu,[28] I. Brock,[21] R. Brock,[89] C. Bromberg,[89] J. Bronner,[100] G. Brooijmans,[35] T. Brooks,[76] W. K. Brooks,[32b] J. Brosamer,[15] E. Brost,[115] G. Brown,[83] J. Brown,[55] P. A. Bruckman de Renstrom,[39] D. Bruncko,[145b] R. Bruneliere,[48] S. Brunet,[60] A. Bruni,[20a] G. Bruni,[20a] M. Bruschi,[20a] L. Bryngemark,[80] T. Buanes,[14] Q. Buat,[143] F. Bucci,[49] P. Buchholz,[142] R. M. Buckingham,[119] A. G. Buckley,[53] S. I. Buda,[26a] I. A. Budagov,[64] F. Buehrer,[48] L. Bugge,[118] M. K. Bugge,[118] O. Bulekov,[97] A. C. Bundock,[73] H. Burckhart,[30] S. Burdin,[73]

B. Burghgrave,[107] S. Burke,[130] I. Burmeister,[43] E. Busato,[34] D. Büscher,[48] V. Büscher,[82] P. Bussey,[53] C. P. Buszello,[167] B. Butler,[57] J. M. Butler,[22] A. I. Butt,[3] C. M. Buttar,[53] J. M. Butterworth,[77] P. Butti,[106] W. Buttinger,[28] A. Buzatu,[53] M. Byszewski,[10] S. Cabrera Urbán,[168] D. Caforio,[20a,20b] O. Cakir,[4a] P. Calafiura,[15] A. Calandri,[137] G. Calderini,[79] P. Calfayan,[99] R. Calkins,[107] L. P. Caloba,[24a] D. Calvet,[34] S. Calvet,[34] R. Camacho Toro,[49] S. Camarda,[42] D. Cameron,[118] L. M. Caminada,[15] R. Caminal Armadans,[12] S. Campana,[30] M. Campanelli,[77] A. Campoverde,[149] V. Canale,[103a,103b] A. Canepa,[160a] M. Cano Bret,[75] J. Cantero,[81] R. Cantrill,[76] T. Cao,[40] M. D. M. Capeans Garrido,[30] I. Caprini,[26a] M. Caprini,[26a] M. Capua,[37a,37b] R. Caputo,[82] R. Cardarelli,[134a] T. Carli,[30] G. Carlino,[103a] L. Carminati,[90a,90b] S. Caron,[105] E. Carquin,[32a] G. D. Carrillo-Montoya,[146c] J. R. Carter,[28] J. Carvalho,[125a,125c] D. Casadei,[77] M. P. Casado,[12] M. Casolino,[12] E. Castaneda-Miranda,[146b] A. Castelli,[106] V. Castillo Gimenez,[168] N. F. Castro,[125a] P. Catastini,[57] A. Catinaccio,[30] J. R. Catmore,[118] A. Cattai,[30] G. Cattani,[134a,134b] S. Caughron,[89] V. Cavaliere,[166] D. Cavalli,[90a] M. Cavalli-Sforza,[12] V. Cavasinni,[123a,123b] F. Ceradini,[135a,135b] B. Cerio,[45] K. Cerny,[128] A. S. Cerqueira,[24b] A. Cerri,[150] L. Cerrito,[75] F. Cerutti,[15] M. Cerv,[30] A. Cervelli,[17] S. A. Cetin,[19b] A. Chafaq,[136a] D. Chakraborty,[107] I. Chalupkova,[128] K. Chan,[3] P. Chang,[166] B. Chapleau,[86] J. D. Chapman,[28] D. Charfeddine,[116] D. G. Charlton,[18] C. C. Chau,[159] C. A. Chavez Barajas,[150] S. Cheatham,[86] A. Chegwidden,[89] S. Chekanov,[6] S. V. Chekulaev,[160a] G. A. Chelkov,[64] M. A. Chelstowska,[88] C. Chen,[63] H. Chen,[25] K. Chen,[149] L. Chen,[33d,h] S. Chen,[33c] X. Chen,[146c] Y. Chen,[35] H. C. Cheng,[88] Y. Cheng,[31] A. Cheplakov,[64] R. Cherkaoui El Moursli,[136e] V. Chernyatin,[25,a] E. Cheu,[7] L. Chevalier,[137] V. Chiarella,[47] G. Chiefari,[103a,103b] J. T. Childers,[6] A. Chilingarov,[71] G. Chiodini,[72a] A. S. Chisholm,[18] R. T. Chislett,[77] A. Chitan,[26a] M. V. Chizhov,[64] S. Chouridou,[9] B. K. B. Chow,[99] D. Chromek-Burckhart,[30] M. L. Chu,[152] J. Chudoba,[126] J. J. Chwastowski,[39] L. Chytka,[114] G. Ciapetti,[133a,133b] A. K. Ciftci,[4a] R. Ciftci,[4a] D. Cinca,[62] V. Cindro,[74] A. Ciocio,[15] P. Cirkovic,[13b] Z. H. Citron,[173] M. Citterio,[90a] M. Ciubancan,[26a] A. Clark,[49] P. J. Clark,[46] R. N. Clarke,[15] W. Cleland,[124] J. C. Clemens,[84] C. Clement,[147a,147b] Y. Coadou,[84] M. Cobal,[165a,165c] A. Coccaro,[139] J. Cochran,[63] L. Coffey,[23] J. G. Cogan,[144] J. Coggeshall,[166] B. Cole,[35] S. Cole,[107] A. P. Colijn,[106] J. Collot,[55] T. Colombo,[58c] G. Colon,[85] G. Compostella,[100] P. Conde Muiño,[125a,125b] E. Coniavitis,[167] M. C. Conidi,[12] S. H. Connell,[146b] I. A. Connelly,[76] S. M. Consonni,[90a,90b] V. Consorti,[48] S. Constantinescu,[26a] C. Conta,[120a,120b] G. Conti,[57] F. Conventi,[103a,i] M. Cooke,[15] B. D. Cooper,[77] A. M. Cooper-Sarkar,[119] N. J. Cooper-Smith,[76] K. Copic,[15] T. Cornelissen,[176] M. Corradi,[20a] F. Corriveau,[86,j] A. Corso-Radu,[164] A. Cortes-Gonzalez,[12] G. Cortiana,[100] G. Costa,[90a] M. J. Costa,[168] D. Costanzo,[140] D. Côté,[8] G. Cottin,[28] G. Cowan,[76] B. E. Cox,[83] K. Cranmer,[109] G. Cree,[29] S. Crépé-Renaudin,[55] F. Crescioli,[79] W. A. Cribbs,[147a,147b] M. Crispin Ortuzar,[119] M. Cristinziani,[21] V. Croft,[105] G. Crosetti,[37a,37b] C.-M. Cuciuc,[26a] T. Cuhadar Donszelmann,[140] J. Cummings,[177] M. Curatolo,[47] C. Cuthbert,[151] H. Czirr,[142] P. Czodrowski,[3] Z. Czyczula,[177] S. D'Auria,[53] M. D'Onofrio,[73] M. J. Da Cunha Sargedas De Sousa,[125a,125b] C. Da Via,[83] W. Dabrowski,[38a] A. Dafinca,[119] T. Dai,[88] O. Dale,[14] F. Dallaire,[94] C. Dallapiccola,[85] M. Dam,[36] A. C. Daniells,[18] M. Dano Hoffmann,[137] V. Dao,[105] G. Darbo,[50a] S. Darmora,[8] J. A. Dassoulas,[42] A. Dattagupta,[60] W. Davey,[21] C. David,[170] T. Davidek,[128] E. Davies,[119,e] M. Davies,[154] O. Davignon,[79] A. R. Davison,[77] P. Davison,[77] Y. Davygora,[58a] E. Dawe,[143] I. Dawson,[140] R. K. Daya-Ishmukhametova,[85] K. De,[8] R. de Asmundis,[103a] S. De Castro,[20a,20b] S. De Cecco,[79] N. De Groot,[105] P. de Jong,[106] H. De la Torre,[81] F. De Lorenzi,[63] L. De Nooij,[106] D. De Pedis,[133a] A. De Salvo,[133a] U. De Sanctis,[165a,165b] A. De Santo,[150] J. B. De Vivie De Regie,[116] W. J. Dearnaley,[71] R. Debbe,[25] C. Debenedetti,[46] B. Dechenaux,[55] D. V. Dedovich,[64] I. Deigaard,[106] J. Del Peso,[81] T. Del Prete,[123a,123b] F. Deliot,[137] C. M. Delitzsch,[49] M. Deliyergiyev,[74] A. Dell'Acqua,[30] L. Dell'Asta,[22] M. Dell'Orso,[123a,123b] M. Della Pietra,[103a,i] D. della Volpe,[49] M. Delmastro,[5] P. A. Delsart,[55] C. Deluca,[106] S. Demers,[177] M. Demichev,[64] A. Demilly,[79] S. P. Denisov,[129] D. Derendarz,[39] J. E. Derkaoui,[136d] F. Derue,[79] P. Dervan,[73] K. Desch,[21] C. Deterre,[42] P. O. Deviveiros,[106] A. Dewhurst,[130] S. Dhaliwal,[106] A. Di Ciaccio,[134a,134b] L. Di Ciaccio,[5] A. Di Domenico,[133a,133b] C. Di Donato,[103a,103b] A. Di Girolamo,[30] B. Di Girolamo,[30] A. Di Mattia,[153] B. Di Micco,[135a,135b] R. Di Nardo,[47] A. Di Simone,[48] R. Di Sipio,[20a,20b] D. Di Valentino,[29] M. A. Diaz,[32a] E. B. Diehl,[88] J. Dietrich,[42] T. A. Dietzsch,[58a] S. Diglio,[84] A. Dimitrievska,[13a] J. Dingfelder,[21] C. Dionisi,[133a,133b] P. Dita,[26a] S. Dita,[26a] F. Dittus,[30] F. Djama,[84] T. Djobava,[51b] M. A. B. do Vale,[24c] A. Do Valle Wemans,[125a,125g] T. K. O. Doan,[5] D. Dobos,[30] C. Doglioni,[49] T. Doherty,[53] T. Dohmae,[156] J. Dolejsi,[128] Z. Dolezal,[128] B. A. Dolgoshein,[97,a] M. Donadelli,[24d] S. Donati,[123a,123b] P. Dondero,[120a,120b] J. Donini,[34] J. Dopke,[30] A. Doria,[103a] M. T. Dova,[70] A. T. Doyle,[53] M. Dris,[10] J. Dubbert,[88] S. Dube,[15] E. Dubreuil,[34] E. Duchovni,[173] G. Duckeck,[99] O. A. Ducu,[26a] D. Duda,[176] A. Dudarev,[30] F. Dudziak,[63] L. Duflot,[116] L. Duguid,[76] M. Dührssen,[30] M. Dunford,[58a] H. Duran Yildiz,[4a] M. Düren,[52] A. Durglishvili,[51b] M. Dwuznik,[38a] M. Dyndal,[38a] J. Ebke,[99] W. Edson,[2] N. C. Edwards,[46] W. Ehrenfeld,[21] T. Eifert,[144] G. Eigen,[14] K. Einsweiler,[15] T. Ekelof,[167]

M. El Kacimi,[136c] M. Ellert,[167] S. Elles,[5] F. Ellinghaus,[82] N. Ellis,[30] J. Elmsheuser,[99] M. Elsing,[30] D. Emeliyanov,[130] Y. Enari,[156] O. C. Endner,[82] M. Endo,[117] R. Engelmann,[149] J. Erdmann,[177] A. Ereditato,[17] D. Eriksson,[147a] G. Ernis,[176] J. Ernst,[2] M. Ernst,[25] J. Ernwein,[137] D. Errede,[166] S. Errede,[166] E. Ertel,[82] M. Escalier,[116] H. Esch,[43] C. Escobar,[124] B. Esposito,[47] A. I. Etienvre,[137] E. Etzion,[154] H. Evans,[60] A. Ezhilov,[122] L. Fabbri,[20a,20b] G. Facini,[31] R. M. Fakhrutdinov,[129] S. Falciano,[133a] R. J. Falla,[77] J. Faltova,[128] Y. Fang,[33a] M. Fanti,[90a,90b] A. Farbin,[8] A. Farilla,[135a] T. Farooque,[12] S. Farrell,[164] S. M. Farrington,[171] P. Farthouat,[30] F. Fassi,[168] P. Fassnacht,[30] D. Fassouliotis,[9] A. Favareto,[50a,50b] L. Fayard,[116] P. Federic,[145a] O. L. Fedin,[122,k] W. Fedorko,[169] M. Fehling-Kaschek,[48] S. Feigl,[30] L. Feligioni,[84] C. Feng,[33d] E. J. Feng,[6] H. Feng,[88] A. B. Fenyuk,[129] S. Fernandez Perez,[30] S. Ferrag,[53] J. Ferrando,[53] A. Ferrari,[167] P. Ferrari,[106] R. Ferrari,[120a] D. E. Ferreira de Lima,[53] A. Ferrer,[168] D. Ferrere,[49] C. Ferretti,[88] A. Ferretto Parodi,[50a,50b] M. Fiascaris,[31] F. Fiedler,[82] A. Filipčič,[74] M. Filipuzzi,[42] F. Filthaut,[105] M. Fincke-Keeler,[170] K. D. Finelli,[151] M. C. N. Fiolhais,[125a,125c] L. Fiorini,[168] A. Firan,[40] J. Fischer,[176] W. C. Fisher,[89] E. A. Fitzgerald,[23] M. Flechl,[48] I. Fleck,[142] P. Fleischmann,[88] S. Fleischmann,[176] G. T. Fletcher,[140] G. Fletcher,[75] T. Flick,[176] A. Floderus,[80] L. R. Flores Castillo,[174] A. C. Florez Bustos,[160b] M. J. Flowerdew,[100] A. Formica,[137] A. Forti,[83] D. Fortin,[160a] D. Fournier,[116] H. Fox,[71] S. Fracchia,[12] P. Francavilla,[79] M. Franchini,[20a,20b] S. Franchino,[30] D. Francis,[30] M. Franklin,[57] S. Franz,[61] M. Fraternali,[120a,120b] S. T. French,[28] C. Friedrich,[42] F. Friedrich,[44] D. Froidevaux,[30] J. A. Frost,[28] C. Fukunaga,[157] E. Fullana Torregrosa,[82] B. G. Fulsom,[144] J. Fuster,[168] C. Gabaldon,[55] O. Gabizon,[173] A. Gabrielli,[20a,20b] A. Gabrielli,[133a,133b] S. Gadatsch,[106] S. Gadomski,[49] G. Gagliardi,[50a,50b] P. Gagnon,[60] C. Galea,[105] B. Galhardo,[125a,125c] E. J. Gallas,[119] V. Gallo,[17] B. J. Gallop,[130] P. Gallus,[127] G. Galster,[36] K. K. Gan,[110] R. P. Gandrajula,[62] J. Gao,[33b,h] Y. S. Gao,[144,g] F. M. Garay Walls,[46] F. Garberson,[177] C. García,[168] J. E. García Navarro,[168] M. Garcia-Sciveres,[15] R. W. Gardner,[31] N. Garelli,[144] V. Garonne,[30] C. Gatti,[47] G. Gaudio,[120a] B. Gaur,[142] L. Gauthier,[94] P. Gauzzi,[133a,133b] I. L. Gavrilenko,[95] C. Gay,[169] G. Gaycken,[21] E. N. Gazis,[10] P. Ge,[33d] Z. Gecse,[169] C. N. P. Gee,[130] D. A. A. Geerts,[106] Ch. Geich-Gimbel,[21] K. Gellerstedt,[147a,147b] C. Gemme,[50a] A. Gemmell,[53] M. H. Genest,[55] S. Gentile,[133a,133b] M. George,[54] S. George,[76] D. Gerbaudo,[164] A. Gershon,[154] H. Ghazlane,[136b] N. Ghodbane,[34] B. Giacobbe,[20a] S. Giagu,[133a,133b] V. Giangiobbe,[12] P. Giannetti,[123a,123b] F. Gianotti,[30] B. Gibbard,[25] S. M. Gibson,[76] M. Gilchriese,[15] T. P. S. Gillam,[28] D. Gillberg,[30] G. Gilles,[34] D. M. Gingrich,[3,f] N. Giokaris,[9] M. P. Giordani,[165a,165c] R. Giordano,[103a,103b] F. M. Giorgi,[20a] F. M. Giorgi,[16] P. F. Giraud,[137] D. Giugni,[90a] C. Giuliani,[48] M. Giulini,[58b] B. K. Gjelsten,[118] S. Gkaitatzis,[155] I. Gkialas,[155,l] L. K. Gladilin,[98] C. Glasman,[81] J. Glatzer,[30] P. C. F. Glaysher,[46] A. Glazov,[42] G. L. Glonti,[64] M. Goblirsch-Kolb,[100] J. R. Goddard,[75] J. Godfrey,[143] J. Godlewski,[30] C. Goeringer,[82] S. Goldfarb,[88] T. Golling,[177] D. Golubkov,[129] A. Gomes,[125a,125b,125d] L. S. Gomez Fajardo,[42] R. Gonçalo,[125a] J. Goncalves Pinto Firmino Da Costa,[137] L. Gonella,[21] S. González de la Hoz,[168] G. Gonzalez Parra,[12] M. L. Gonzalez Silva,[27] S. Gonzalez-Sevilla,[49] L. Goossens,[30] P. A. Gorbounov,[96] H. A. Gordon,[25] I. Gorelov,[104] B. Gorini,[30] E. Gorini,[72a,72b] A. Gorišek,[74] E. Gornicki,[39] A. T. Goshaw,[6] C. Gössling,[43] M. I. Gostkin,[64] M. Gouighri,[136a] D. Goujdami,[136c] M. P. Goulette,[49] A. G. Goussiou,[139] C. Goy,[5] S. Gozpinar,[23] H. M. X. Grabas,[137] L. Graber,[54] I. Grabowska-Bold,[38a] P. Grafström,[20a,20b] K-J. Grahn,[42] J. Gramling,[49] E. Gramstad,[118] S. Grancagnolo,[16] V. Grassi,[149] V. Gratchev,[122] H. M. Gray,[30] E. Graziani,[135a] O. G. Grebenyuk,[122] Z. D. Greenwood,[78,m] K. Gregersen,[77] I. M. Gregor,[42] P. Grenier,[144] J. Griffiths,[8] A. A. Grillo,[138] K. Grimm,[71] S. Grinstein,[12,n] Ph. Gris,[34] Y. V. Grishkevich,[98] J.-F. Grivaz,[116] J. P. Grohs,[44] A. Grohsjean,[42] E. Gross,[173] J. Grosse-Knetter,[54] G. C. Grossi,[134a,134b] J. Groth-Jensen,[173] Z. J. Grout,[150] L. Guan,[33b] F. Guescini,[49] D. Guest,[177] O. Gueta,[154] C. Guicheney,[34] E. Guido,[50a,50b] T. Guillemin,[116] S. Guindon,[2] U. Gul,[53] C. Gumpert,[44] J. Gunther,[127] J. Guo,[35] S. Gupta,[119] P. Gutierrez,[112] N. G. Gutierrez Ortiz,[53] C. Gutschow,[77] N. Guttman,[154] C. Guyot,[137] C. Gwenlan,[119] C. B. Gwilliam,[73] A. Haas,[109] C. Haber,[15] H. K. Hadavand,[8] N. Haddad,[136e] P. Haefner,[21] S. Hageboeck,[21] Z. Hajduk,[39] H. Hakobyan,[178] M. Haleem,[42] D. Hall,[119] G. Halladjian,[89] K. Hamacher,[176] P. Hamal,[114] K. Hamano,[170] M. Hamer,[54] A. Hamilton,[146a] S. Hamilton,[162] P. G. Hamnett,[42] L. Han,[33b] K. Hanagaki,[117] K. Hanawa,[156] M. Hance,[15] P. Hanke,[58a] R. Hanna,[137] J. B. Hansen,[36] J. D. Hansen,[36] P. H. Hansen,[36] K. Hara,[161] A. S. Hard,[174] T. Harenberg,[176] S. Harkusha,[91] D. Harper,[88] R. D. Harrington,[46] O. M. Harris,[139] P. F. Harrison,[171] F. Hartjes,[106] S. Hasegawa,[102] Y. Hasegawa,[141] A. Hasib,[112] S. Hassani,[137] S. Haug,[17] M. Hauschild,[30] R. Hauser,[89] M. Havranek,[126] C. M. Hawkes,[18] R. J. Hawkings,[30] A. D. Hawkins,[80] T. Hayashi,[161] D. Hayden,[89] C. P. Hays,[119] H. S. Hayward,[73] S. J. Haywood,[130] S. J. Head,[18] T. Heck,[82] V. Hedberg,[80] L. Heelan,[8] S. Heim,[121] T. Heim,[176] B. Heinemann,[15] L. Heinrich,[109] S. Heisterkamp,[36] J. Hejbal,[126] L. Helary,[22] C. Heller,[99] M. Heller,[30] S. Hellman,[147a,147b] D. Hellmich,[21] C. Helsens,[30] J. Henderson,[119] R. C. W. Henderson,[71] C. Hengler,[42] A. Henrichs,[177] A. M. Henriques Correia,[30] S. Henrot-Versille,[116] C. Hensel,[54] G. H. Herbert,[16] Y. Hernández Jiménez,[168] R. Herrberg-Schubert,[16] G. Herten,[48]

R. Hertenberger,[99] L. Hervas,[30] G. G. Hesketh,[77] N. P. Hessey,[106] R. Hickling,[75] E. Higón-Rodriguez,[168] E. Hill,[170] J. C. Hill,[28] K. H. Hiller,[42] S. Hillert,[21] S. J. Hillier,[18] I. Hinchliffe,[15] E. Hines,[121] M. Hirose,[158] D. Hirschbuehl,[176] J. Hobbs,[149] N. Hod,[106] M. C. Hodgkinson,[140] P. Hodgson,[140] A. Hoecker,[30] M. R. Hoeferkamp,[104] J. Hoffman,[40] D. Hoffmann,[84] J. I. Hofmann,[58a] M. Hohlfeld,[82] T. R. Holmes,[15] T. M. Hong,[121] L. Hooft van Huysduynen,[109] J-Y. Hostachy,[55] S. Hou,[152] A. Hoummada,[136a] J. Howard,[119] J. Howarth,[42] M. Hrabovsky,[114] I. Hristova,[16] J. Hrivnac,[116] T. Hryn'ova,[5] P. J. Hsu,[82] S.-C. Hsu,[139] D. Hu,[35] X. Hu,[25] Y. Huang,[42] Z. Hubacek,[30] F. Hubaut,[84] F. Huegging,[21] T. B. Huffman,[119] E. W. Hughes,[35] G. Hughes,[71] M. Huhtinen,[30] T. A. Hülsing,[82] M. Hurwitz,[15] N. Huseynov,[64,c] J. Huston,[89] J. Huth,[57] G. Iacobucci,[49] G. Iakovidis,[10] I. Ibragimov,[142] L. Iconomidou-Fayard,[116] E. Ideal,[177] P. Iengo,[103a] O. Igonkina,[106] T. Iizawa,[172] Y. Ikegami,[65] K. Ikematsu,[142] M. Ikeno,[65] Y. Ilchenko,[31,bb] D. Iliadis,[155] N. Ilic,[159] Y. Inamaru,[66] T. Ince,[100] P. Ioannou,[9] M. Iodice,[135a] K. Iordanidou,[9] V. Ippolito,[57] A. Irles Quiles,[168] C. Isaksson,[167] M. Ishino,[67] M. Ishitsuka,[158] R. Ishmukhametov,[110] C. Issever,[119] S. Istin,[19a] J. M. Iturbe Ponce,[83] R. Iuppa,[134a,134b] J. Ivarsson,[80] W. Iwanski,[39] H. Iwasaki,[65] J. M. Izen,[41] V. Izzo,[103a] B. Jackson,[121] M. Jackson,[73] P. Jackson,[1] M. R. Jaekel,[30] V. Jain,[2] K. Jakobs,[48] S. Jakobsen,[30] T. Jakoubek,[126] J. Jakubek,[127] D. O. Jamin,[152] D. K. Jana,[78] E. Jansen,[77] H. Jansen,[30] J. Janssen,[21] M. Janus,[171] G. Jarlskog,[80] N. Javadov,[64,c] T. Javůrek,[48] L. Jeanty,[15] J. Jejelava,[51a,o] G. -Y. Jeng,[151] D. Jennens,[87] P. Jenni,[48,p] J. Jentzsch,[43] C. Jeske,[171] S. Jézéquel,[5] H. Ji,[174] W. Ji,[82] J. Jia,[149] Y. Jiang,[33b] M. Jimenez Belenguer,[42] S. Jin,[33a] A. Jinaru,[26a] O. Jinnouchi,[158] M. D. Joergensen,[36] K. E. Johansson,[147a] P. Johansson,[140] K. A. Johns,[7] K. Jon-And,[147a,147b] G. Jones,[171] R. W. L. Jones,[71] T. J. Jones,[73] J. Jongmanns,[58a] P. M. Jorge,[125a,125b] K. D. Joshi,[83] J. Jovicevic,[148] X. Ju,[174] C. A. Jung,[43] R. M. Jungst,[30] P. Jussel,[61] A. Juste Rozas,[12,n] M. Kaci,[168] A. Kaczmarska,[39] M. Kado,[116] H. Kagan,[110] M. Kagan,[144] E. Kajomovitz,[45] C. W. Kalderon,[119] S. Kama,[40] N. Kanaya,[156] M. Kaneda,[30] S. Kaneti,[28] T. Kanno,[158] V. A. Kantserov,[97] J. Kanzaki,[65] B. Kaplan,[109] A. Kapliy,[31] D. Kar,[53] K. Karakostas,[10] N. Karastathis,[10] M. Karnevskiy,[82] S. N. Karpov,[64] K. Karthik,[109] V. Kartvelishvili,[71] A. N. Karyukhin,[129] L. Kashif,[174] G. Kasieczka,[58b] R. D. Kass,[110] A. Kastanas,[14] Y. Kataoka,[156] A. Katre,[49] J. Katzy,[42] V. Kaushik,[7] K. Kawagoe,[69] T. Kawamoto,[156] G. Kawamura,[54] S. Kazama,[156] V. F. Kazanin,[108] M. Y. Kazarinov,[64] R. Keeler,[170] R. Kehoe,[40] M. Keil,[54] J. S. Keller,[42] J. J. Kempster,[76] H. Keoshkerian,[5] O. Kepka,[126] B. P. Kerševan,[74] S. Kersten,[176] K. Kessoku,[156] J. Keung,[159] F. Khalil-zada,[11] H. Khandanyan,[147a,147b] A. Khanov,[113] A. Khodinov,[97] A. Khomich,[58a] T. J. Khoo,[28] G. Khoriauli,[21] A. Khoroshilov,[176] V. Khovanskiy,[96] E. Khramov,[64] J. Khubua,[51b] H. Y. Kim,[8] H. Kim,[147a,147b] S. H. Kim,[161] N. Kimura,[172] O. Kind,[16] B. T. King,[73] M. King,[168] R. S. B. King,[119] S. B. King,[169] J. Kirk,[130] A. E. Kiryunin,[100] T. Kishimoto,[66] D. Kisielewska,[38a] F. Kiss,[48] T. Kitamura,[66] T. Kittelmann,[124] K. Kiuchi,[161] E. Kladiva,[145b] M. Klein,[73] U. Klein,[73] K. Kleinknecht,[82] P. Klimek,[147a,147b] A. Klimentov,[25] R. Klingenberg,[43] J. A. Klinger,[83] T. Klioutchnikova,[30] P. F. Klok,[105] E.-E. Kluge,[58a] P. Kluit,[106] S. Kluth,[100] E. Kneringer,[61] E. B. F. G. Knoops,[84] A. Knue,[53] T. Kobayashi,[156] M. Kobel,[44] M. Kocian,[144] P. Kodys,[128] P. Koevesarki,[21] T. Koffas,[29] E. Koffeman,[106] L. A. Kogan,[119] S. Kohlmann,[176] Z. Kohout,[127] T. Kohriki,[65] T. Koi,[144] H. Kolanoski,[16] I. Koletsou,[5] J. Koll,[89] A. A. Komar,[95,a] Y. Komori,[156] T. Kondo,[65] N. Kondrashova,[42] K. Köneke,[48] A. C. König,[105] S. König,[82] T. Kono,[65,q] R. Konoplich,[109,r] N. Konstantinidis,[77] R. Kopeliansky,[153] S. Koperny,[38a] L. Köpke,[82] A. K. Kopp,[48] K. Korcyl,[39] K. Kordas,[155] A. Korn,[77] A. A. Korol,[108,s] I. Korolkov,[12] E. V. Korolkova,[140] V. A. Korotkov,[129] O. Kortner,[100] S. Kortner,[100] V. V. Kostyukhin,[21] V. M. Kotov,[64] A. Kotwal,[45] C. Kourkoumelis,[9] V. Kouskoura,[155] A. Koutsman,[160a] R. Kowalewski,[170] T. Z. Kowalski,[38a] W. Kozanecki,[137] A. S. Kozhin,[129] V. Kral,[127] V. A. Kramarenko,[98] G. Kramberger,[74] D. Krasnopevtsev,[97] M. W. Krasny,[79] A. Krasznahorkay,[30] J. K. Kraus,[21] A. Kravchenko,[25] S. Kreiss,[109] M. Kretz,[58c] J. Kretzschmar,[73] K. Kreutzfeldt,[52] P. Krieger,[159] K. Kroeninger,[54] H. Kroha,[100] J. Kroll,[121] J. Kroseberg,[21] J. Krstic,[13a] U. Kruchonak,[64] H. Krüger,[21] T. Kruker,[17] N. Krumnack,[63] Z. V. Krumshteyn,[64] A. Kruse,[174] M. C. Kruse,[45] M. Kruskal,[22] T. Kubota,[87] S. Kuday,[4a] S. Kuehn,[48] A. Kugel,[58c] A. Kuhl,[138] T. Kuhl,[42] V. Kukhtin,[64] Y. Kulchitsky,[91] S. Kuleshov,[32b] M. Kuna,[133a,133b] J. Kunkle,[121] A. Kupco,[126] H. Kurashige,[66] Y. A. Kurochkin,[91] R. Kurumida,[66] V. Kus,[126] E. S. Kuwertz,[148] M. Kuze,[158] J. Kvita,[114] A. La Rosa,[49] L. La Rotonda,[37a,37b] C. Lacasta,[168] F. Lacava,[133a,133b] J. Lacey,[29] H. Lacker,[16] D. Lacour,[79] V. R. Lacuesta,[168] E. Ladygin,[64] R. Lafaye,[5] B. Laforge,[79] T. Lagouri,[177] S. Lai,[48] H. Laier,[58a] L. Lambourne,[77] S. Lammers,[60] C. L. Lampen,[7] W. Lampl,[7] E. Lançon,[137] U. Landgraf,[48] M. P. J. Landon,[75] V. S. Lang,[58a] C. Lange,[42] A. J. Lankford,[164] F. Lanni,[25] K. Lantzsch,[30] S. Laplace,[79] C. Lapoire,[21] J. F. Laporte,[137] T. Lari,[90a] M. Lassnig,[30] P. Laurelli,[47] W. Lavrijsen,[15] A. T. Law,[138] P. Laycock,[73] B. T. Le,[55] O. Le Dortz,[79] E. Le Guirriec,[84] E. Le Menedeu,[12] T. LeCompte,[6] F. Ledroit-Guillon,[55] C. A. Lee,[152] H. Lee,[106] J. S. H. Lee,[117] S. C. Lee,[152] L. Lee,[177] G. Lefebvre,[79] M. Lefebvre,[170] F. Legger,[99] C. Leggett,[15] A. Lehan,[73] M. Lehmacher,[21] G. Lehmann Miotto,[30] X. Lei,[7] W. A. Leight,[29] A. Leisos,[155]

A. G. Leister,[177] M. A. L. Leite,[24d] R. Leitner,[128] D. Lellouch,[173] B. Lemmer,[54] K. J. C. Leney,[77] T. Lenz,[106] G. Lenzen,[176] B. Lenzi,[30] R. Leone,[7] K. Leonhardt,[44] S. Leontsinis,[10] C. Leroy,[94] C. G. Lester,[28] C. M. Lester,[121] M. Levchenko,[122] J. Levêque,[5] D. Levin,[88] L. J. Levinson,[173] M. Levy,[18] A. Lewis,[119] G. H. Lewis,[109] A. M. Leyko,[21] M. Leyton,[41] B. Li,[33b,t] B. Li,[84] H. Li,[149] H. L. Li,[31] L. Li,[45] L. Li,[33e] S. Li,[45] Y. Li,[33c,u] Z. Liang,[138] H. Liao,[34] B. Liberti,[134a] P. Lichard,[30] K. Lie,[166] J. Liebal,[21] W. Liebig,[14] C. Limbach,[21] A. Limosani,[87] S. C. Lin,[152,v] F. Linde,[106] B. E. Lindquist,[149] J. T. Linnemann,[89] E. Lipeles,[121] A. Lipniacka,[14] M. Lisovyi,[42] T. M. Liss,[166] D. Lissauer,[25] A. Lister,[169] A. M. Litke,[138] B. Liu,[152] D. Liu,[152] J. B. Liu,[33b] K. Liu,[33b,w] L. Liu,[88] M. Liu,[45] M. Liu,[33b] Y. Liu,[33b] M. Livan,[120a,120b] S. S. A. Livermore,[119] A. Lleres,[55] J. Llorente Merino,[81] S. L. Lloyd,[75] F. Lo Sterzo,[152] E. Lobodzinska,[42] P. Loch,[7] W. S. Lockman,[138] T. Loddenkoetter,[21] F. K. Loebinger,[83] A. E. Loevschall-Jensen,[36] A. Loginov,[177] C. W. Loh,[169] T. Lohse,[16] K. Lohwasser,[42] M. Lokajicek,[126] V. P. Lombardo,[5] B. A. Long,[22] J. D. Long,[88] R. E. Long,[71] L. Lopes,[125a] D. Lopez Mateos,[57] B. Lopez Paredes,[140] I. Lopez Paz,[12] J. Lorenz,[99] N. Lorenzo Martinez,[60] M. Losada,[163] P. Loscutoff,[15] X. Lou,[41] A. Lounis,[116] J. Love,[6] P. A. Love,[71] A. J. Lowe,[144,g] F. Lu,[33a] H. J. Lubatti,[139] C. Luci,[133a,133b] A. Lucotte,[55] F. Luehring,[60] W. Lukas,[61] L. Luminari,[133a] O. Lundberg,[147a,147b] B. Lund-Jensen,[148] M. Lungwitz,[82] D. Lynn,[25] R. Lysak,[126] E. Lytken,[80] H. Ma,[25] L. L. Ma,[33d] G. Maccarrone,[47] A. Macchiolo,[100] J. Machado Miguens,[125a,125b] D. Macina,[30] D. Madaffari,[84] R. Madar,[48] H. J. Maddocks,[71] W. F. Mader,[44] A. Madsen,[167] M. Maeno,[8] T. Maeno,[25] E. Magradze,[54] K. Mahboubi,[48] J. Mahlstedt,[106] S. Mahmoud,[73] C. Maiani,[137] C. Maidantchik,[24a] A. Maio,[125a,125b,125d] S. Majewski,[115] Y. Makida,[65] N. Makovec,[116] P. Mal,[137,x] B. Malaescu,[79] Pa. Malecki,[39] V. P. Maleev,[122] F. Malek,[55] U. Mallik,[62] D. Malon,[6] C. Malone,[144] S. Maltezos,[10] V. M. Malyshev,[108] S. Malyukov,[30] J. Mamuzic,[13b] B. Mandelli,[30] L. Mandelli,[90a] I. Mandić,[74] R. Mandrysch,[62] J. Maneira,[125a,125b] A. Manfredini,[100] L. Manhaes de Andrade Filho,[24b] J. A. Manjarres Ramos,[160b] A. Mann,[99] P. M. Manning,[138] A. Manousakis-Katsikakis,[9] B. Mansoulie,[137] R. Mantifel,[86] L. Mapelli,[30] L. March,[168] J. F. Marchand,[29] G. Marchiori,[79] M. Marcisovsky,[126] C. P. Marino,[170] M. Marjanovic,[13a] C. N. Marques,[125a] F. Marroquim,[24a] S. P. Marsden,[83] Z. Marshall,[15] L. F. Marti,[17] S. Marti-Garcia,[168] B. Martin,[30] B. Martin,[89] T. A. Martin,[171] V. J. Martin,[46] B. Martin dit Latour,[14] H. Martinez,[137] M. Martinez,[12,n] S. Martin-Haugh,[130] A. C. Martyniuk,[77] M. Marx,[139] F. Marzano,[133a] A. Marzin,[30] L. Masetti,[82] T. Mashimo,[156] R. Mashinistov,[95] J. Masik,[83] A. L. Maslennikov,[108] I. Massa,[20a,20b] N. Massol,[5] P. Mastrandrea,[149] A. Mastroberardino,[37a,37b] T. Masubuchi,[156] T. Matsushita,[66] P. Mättig,[176] S. Mättig,[42] J. Mattmann,[82] J. Maurer,[26a] S. J. Maxfield,[73] D. A. Maximov,[108,s] R. Mazini,[152] L. Mazzaferro,[134a,134b] G. Mc Goldrick,[159] S. P. Mc Kee,[88] A. McCarn,[88] R. L. McCarthy,[149] T. G. McCarthy,[29] N. A. McCubbin,[130] K. W. McFarlane,[56,a] J. A. Mcfayden,[77] G. Mchedlidze,[54] S. J. McMahon,[130] R. A. McPherson,[170,j] A. Meade,[85] J. Mechnich,[106] M. Medinnis,[42] S. Meehan,[31] S. Mehlhase,[36] A. Mehta,[73] K. Meier,[58a] C. Meineck,[99] B. Meirose,[80] C. Melachrinos,[31] B. R. Mellado Garcia,[146c] F. Meloni,[90a,90b] A. Mengarelli,[20a,20b] S. Menke,[100] E. Meoni,[162] K. M. Mercurio,[57] S. Mergelmeyer,[21] N. Meric,[137] P. Mermod,[49] L. Merola,[103a,103b] C. Meroni,[90a] F. S. Merritt,[31] H. Merritt,[110] A. Messina,[30,y] J. Metcalfe,[25] A. S. Mete,[164] C. Meyer,[82] C. Meyer,[31] J-P. Meyer,[137] J. Meyer,[30] R. P. Middleton,[130] S. Migas,[73] L. Mijović,[21] G. Mikenberg,[173] M. Mikestikova,[126] M. Mikuž,[74] D. W. Miller,[31] C. Mills,[46] A. Milov,[173] D. A. Milstead,[147a,147b] D. Milstein,[173] A. A. Minaenko,[129] I. A. Minashvili,[64] A. I. Mincer,[109] B. Mindur,[38a] M. Mineev,[64] Y. Ming,[174] L. M. Mir,[12] G. Mirabelli,[133a] T. Mitani,[172] J. Mitrevski,[99] V. A. Mitsou,[168] S. Mitsui,[65] A. Miucci,[49] P. S. Miyagawa,[140] J. U. Mjörnmark,[80] T. Moa,[147a,147b] K. Mochizuki,[84] V. Moeller,[28] S. Mohapatra,[35] W. Mohr,[48] S. Molander,[147a,147b] R. Moles-Valls,[168] K. Mönig,[42] C. Monini,[55] J. Monk,[36] E. Monnier,[84] J. Montejo Berlingen,[12] F. Monticelli,[70] S. Monzani,[133a,133b] R. W. Moore,[3] A. Moraes,[53] N. Morange,[62] D. Moreno,[82] M. Moreno Llácer,[54] P. Morettini,[50a] M. Morgenstern,[44] M. Morii,[57] S. Moritz,[82] A. K. Morley,[148] G. Mornacchi,[30] J. D. Morris,[75] L. Morvaj,[102] H. G. Moser,[100] M. Mosidze,[51b] J. Moss,[110] R. Mount,[144] E. Mountricha,[25] S. V. Mouraviev,[95,a] E. J. W. Moyse,[85] S. Muanza,[84] R. D. Mudd,[18] F. Mueller,[58a] J. Mueller,[124] K. Mueller,[21] T. Mueller,[28] T. Mueller,[82] D. Muenstermann,[49] Y. Munwes,[154] J. A. Murillo Quijada,[18] W. J. Murray,[171,130] H. Musheghyan,[54] E. Musto,[153] A. G. Myagkov,[129,z] M. Myska,[127] O. Nackenhorst,[54] J. Nadal,[54] K. Nagai,[61] R. Nagai,[158] Y. Nagai,[84] K. Nagano,[65] A. Nagarkar,[110] Y. Nagasaka,[59] M. Nagel,[100] A. M. Nairz,[30] Y. Nakahama,[30] K. Nakamura,[65] T. Nakamura,[156] I. Nakano,[111] H. Namasivayam,[41] G. Nanava,[21] R. Narayan,[58b] T. Nattermann,[21] T. Naumann,[42] G. Navarro,[163] R. Nayyar,[7] H. A. Neal,[88] P. Yu. Nechaeva,[95] T. J. Neep,[83] A. Negri,[120a,120b] G. Negri,[30] M. Negrini,[20a] S. Nektarijevic,[49] A. Nelson,[164] T. K. Nelson,[144] S. Nemecek,[126] P. Nemethy,[109] A. A. Nepomuceno,[24a] M. Nessi,[30,aa] M. S. Neubauer,[166] M. Neumann,[176] R. M. Neves,[109] P. Nevski,[25] P. R. Newman,[18] D. H. Nguyen,[6] R. B. Nickerson,[119] R. Nicolaidou,[137] B. Nicquevert,[30] J. Nielsen,[138] N. Nikiforou,[35] A. Nikiforov,[16] V. Nikolaenko,[129,z] I. Nikolic-Audit,[79] K. Nikolics,[49] K. Nikolopoulos,[18] P. Nilsson,[8] Y. Ninomiya,[156] A. Nisati,[133a] R. Nisius,[100] T. Nobe,[158] L. Nodulman,[6]

M. Nomachi,[117] I. Nomidis,[155] S. Norberg,[112] M. Nordberg,[30] S. Nowak,[100] M. Nozaki,[65] L. Nozka,[114] K. Ntekas,[10] G. Nunes Hanninger,[87] T. Nunnemann,[99] E. Nurse,[77] F. Nuti,[87] B. J. O'Brien,[46] F. O'grady,[7] D. C. O'Neil,[143] V. O'Shea,[53] F. G. Oakham,[29,f] H. Oberlack,[100] T. Obermann,[21] J. Ocariz,[79] A. Ochi,[66] M. I. Ochoa,[77] S. Oda,[69] S. Odaka,[65] H. Ogren,[60] A. Oh,[83] S. H. Oh,[45] C. C. Ohm,[30] H. Ohman,[167] T. Ohshima,[102] W. Okamura,[117] H. Okawa,[25] Y. Okumura,[31] T. Okuyama,[156] A. Olariu,[26a] A. G. Olchevski,[64] S. A. Olivares Pino,[46] D. Oliveira Damazio,[25] E. Oliver Garcia,[168] A. Olszewski,[39] J. Olszowska,[39] A. Onofre,[125a,125e] P. U. E. Onyisi,[31,bb] C. J. Oram,[160a] M. J. Oreglia,[31] Y. Oren,[154] D. Orestano,[135a,135b] N. Orlando,[72a,72b] C. Oropeza Barrera,[53] R. S. Orr,[159] B. Osculati,[50a,50b] R. Ospanov,[121] G. Otero y Garzon,[27] H. Otono,[69] M. Ouchrif,[136d] E. A. Ouellette,[170] F. Ould-Saada,[118] A. Ouraou,[137] K. P. Oussoren,[106] Q. Ouyang,[33a] A. Ovcharova,[15] M. Owen,[83] V. E. Ozcan,[19a] N. Ozturk,[8] K. Pachal,[119] A. Pacheco Pages,[12] C. Padilla Aranda,[12] M. Pagáčová,[48] S. Pagan Griso,[15] E. Paganis,[140] C. Pahl,[100] F. Paige,[25] P. Pais,[85] K. Pajchel,[118] G. Palacino,[160b] S. Palestini,[30] M. Palka,[38b] D. Pallin,[34] A. Palma,[125a,125b] J. D. Palmer,[18] Y. B. Pan,[174] E. Panagiotopoulou,[10] J. G. Panduro Vazquez,[76] P. Pani,[106] N. Panikashvili,[88] S. Panitkin,[25] D. Pantea,[26a] L. Paolozzi,[134a,134b] Th. D. Papadopoulou,[10] K. Papageorgiou,[155,l] A. Paramonov,[6] D. Paredes Hernandez,[34] M. A. Parker,[28] F. Parodi,[50a,50b] J. A. Parsons,[35] U. Parzefall,[48] E. Pasqualucci,[133a] S. Passaggio,[50a] A. Passeri,[135a] F. Pastore,[135a,135b,a] Fr. Pastore,[76] G. Pásztor,[29] S. Pataraia,[176] N. D. Patel,[151] J. R. Pater,[83] S. Patricelli,[103a,103b] T. Pauly,[30] J. Pearce,[170] M. Pedersen,[118] S. Pedraza Lopez,[168] R. Pedro,[125a,125b] S. V. Peleganchuk,[108] D. Pelikan,[167] H. Peng,[33b] B. Penning,[31] J. Penwell,[60] D. V. Perepelitsa,[25] E. Perez Codina,[160a] M. T. Pérez García-Estañ,[168] V. Perez Reale,[35] L. Perini,[90a,90b] H. Pernegger,[30] R. Perrino,[72a] R. Peschke,[42] V. D. Peshekhonov,[64] K. Peters,[30] R. F. Y. Peters,[83] B. A. Petersen,[87] T. C. Petersen,[36] E. Petit,[42] A. Petridis,[147a,147b] C. Petridou,[155] E. Petrolo,[133a] F. Petrucci,[135a,135b] M. Petteni,[143] N. E. Pettersson,[158] R. Pezoa,[32b] P. W. Phillips,[130] G. Piacquadio,[144] E. Pianori,[171] A. Picazio,[49] E. Piccaro,[75] M. Piccinini,[20a,20b] R. Piegaia,[27] D. T. Pignotti,[110] J. E. Pilcher,[31] A. D. Pilkington,[77] J. Pina,[125a,125b,125d] M. Pinamonti,[165a,165c,cc] A. Pinder,[119] J. L. Pinfold,[3] A. Pingel,[36] B. Pinto,[125a] S. Pires,[79] M. Pitt,[173] C. Pizio,[90a,90b] L. Plazak,[145a] M. -A. Pleier,[25] V. Pleskot,[128] E. Plotnikova,[64] P. Plucinski,[147a,147b] S. Poddar,[58a] F. Podlyski,[34] R. Poettgen,[82] L. Poggioli,[116] D. Pohl,[21] M. Pohl,[49] G. Polesello,[120a] A. Policicchio,[37a,37b] R. Polifka,[159] A. Polini,[20a] C. S. Pollard,[45] V. Polychronakos,[25] K. Pommès,[30] L. Pontecorvo,[133a] B. G. Pope,[89] G. A. Popeneciu,[26b] D. S. Popovic,[13a] A. Poppleton,[30] X. Portell Bueso,[12] G. E. Pospelov,[100] S. Pospisil,[127] K. Potamianos,[15] I. N. Potrap,[64] C. J. Potter,[150] C. T. Potter,[115] G. Poulard,[30] J. Poveda,[60] V. Pozdnyakov,[64] P. Pralavorio,[84] A. Pranko,[15] S. Prasad,[30] R. Pravahan,[8] S. Prell,[63] D. Price,[83] J. Price,[73] L. E. Price,[6] D. Prieur,[124] M. Primavera,[72a] M. Proissl,[46] K. Prokofiev,[47] F. Prokoshin,[32b] E. Protopapadaki,[137] S. Protopopescu,[25] J. Proudfoot,[6] M. Przybycien,[38a] H. Przysiezniak,[5] E. Ptacek,[115] E. Pueschel,[85] D. Puldon,[149] M. Purohit,[25,dd] P. Puzo,[116] J. Qian,[88] G. Qin,[53] Y. Qin,[83] A. Quadt,[54] D. R. Quarrie,[15] W. B. Quayle,[165a,165b] M. Queitsch-Maitland,[83] D. Quilty,[53] A. Qureshi,[160b] V. Radeka,[25] V. Radescu,[42] S. K. Radhakrishnan,[149] P. Radloff,[115] P. Rados,[87] F. Ragusa,[90a,90b] G. Rahal,[179] S. Rajagopalan,[25] M. Rammensee,[30] A. S. Randle-Conde,[40] C. Rangel-Smith,[167] K. Rao,[164] F. Rauscher,[99] S. Rave,[82] T. C. Rave,[48] T. Ravenscroft,[53] M. Raymond,[30] A. L. Read,[118] N. P. Readioff,[73] D. M. Rebuzzi,[120a,120b] A. Redelbach,[175] G. Redlinger,[25] R. Reece,[138] K. Reeves,[41] L. Rehnisch,[16] H. Reisin,[27] M. Relich,[164] C. Rembser,[30] H. Ren,[33a] Z. L. Ren,[152] A. Renaud,[116] M. Rescigno,[133a] S. Resconi,[90a] O. L. Rezanova,[108,s] P. Reznicek,[128] R. Rezvani,[94] R. Richter,[100] M. Ridel,[79] P. Rieck,[16] J. Rieger,[54] M. Rijssenbeek,[149] A. Rimoldi,[120a,120b] L. Rinaldi,[20a] E. Ritsch,[61] I. Riu,[12] F. Rizatdinova,[113] E. Rizvi,[75] S. H. Robertson,[86,j] A. Robichaud-Veronneau,[86] D. Robinson,[28] J. E. M. Robinson,[83] A. Robson,[53] C. Roda,[123a,123b] L. Rodrigues,[30] S. Roe,[30] O. Røhne,[118] S. Rolli,[162] A. Romaniouk,[97] M. Romano,[20a,20b] G. Romeo,[27] E. Romero Adam,[168] N. Rompotis,[139] L. Roos,[79] E. Ros,[168] S. Rosati,[133a] K. Rosbach,[49] M. Rose,[76] P. L. Rosendahl,[14] O. Rosenthal,[142] V. Rossetti,[147a,147b] E. Rossi,[103a,103b] L. P. Rossi,[50a] R. Rosten,[139] M. Rotaru,[26a] I. Roth,[173] J. Rothberg,[139] D. Rousseau,[116] C. R. Royon,[137] A. Rozanov,[84] Y. Rozen,[153] X. Ruan,[146c] F. Rubbo,[12] I. Rubinskiy,[42] V. I. Rud,[98] C. Rudolph,[44] M. S. Rudolph,[159] F. Rühr,[48] A. Ruiz-Martinez,[30] Z. Rurikova,[48] N. A. Rusakovich,[64] A. Ruschke,[99] J. P. Rutherfoord,[7] N. Ruthmann,[48] Y. F. Ryabov,[122] M. Rybar,[128] G. Rybkin,[116] N. C. Ryder,[119] A. F. Saavedra,[151] S. Sacerdoti,[27] A. Saddique,[3] I. Sadeh,[154] H. F-W. Sadrozinski,[138] R. Sadykov,[64] F. Safai Tehrani,[133a] H. Sakamoto,[156] Y. Sakurai,[172] G. Salamanna,[75] A. Salamon,[134a] M. Saleem,[112] D. Salek,[106] P. H. Sales De Bruin,[139] D. Salihagic,[100] A. Salnikov,[144] J. Salt,[168] B. M. Salvachua Ferrando,[6] D. Salvatore,[37a,37b] F. Salvatore,[150] A. Salvucci,[105] A. Salzburger,[30] D. Sampsonidis,[155] A. Sanchez,[103a,103b] J. Sánchez,[168] V. Sanchez Martinez,[168] H. Sandaker,[14] R. L. Sandbach,[75] H. G. Sander,[82] M. P. Sanders,[99] M. Sandhoff,[176] T. Sandoval,[28] C. Sandoval,[163] R. Sandstroem,[100] D. P. C. Sankey,[130] F. Sannino,[ee] A. Sansoni,[47] C. Santoni,[34] R. Santonico,[134a,134b] H. Santos,[125a] I. Santoyo Castillo,[150] K. Sapp,[124] A. Sapronov,[64]

J. G. Saraiva,[125a,125d] B. Sarrazin,[21] G. Sartisohn,[176] O. Sasaki,[65] Y. Sasaki,[156] G. Sauvage,[5,a] E. Sauvan,[5] P. Savard,[159,f] D. O. Savu,[30] C. Sawyer,[119] L. Sawyer,[78,m] D. H. Saxon,[53] J. Saxon,[121] C. Sbarra,[20a] A. Sbrizzi,[3] T. Scanlon,[77] D. A. Scannicchio,[164] M. Scarcella,[151] J. Schaarschmidt,[173] P. Schacht,[100] D. Schaefer,[121] R. Schaefer,[42] S. Schaepe,[21] S. Schaetzel,[58b] U. Schäfer,[82] A. C. Schaffer,[116] D. Schaile,[99] R. D. Schamberger,[149] V. Scharf,[58a] V. A. Schegelsky,[122] D. Scheirich,[128] M. Schernau,[164] M. I. Scherzer,[35] C. Schiavi,[50a,50b] J. Schieck,[99] C. Schillo,[48] M. Schioppa,[37a,37b] S. Schlenker,[30] E. Schmidt,[48] K. Schmieden,[30] C. Schmitt,[82] C. Schmitt,[99] S. Schmitt,[58b] B. Schneider,[17] Y. J. Schnellbach,[73] U. Schnoor,[44] L. Schoeffel,[137] A. Schoening,[58b] B. D. Schoenrock,[89] A. L. S. Schorlemmer,[54] M. Schott,[82] D. Schouten,[160a] J. Schovancova,[25] S. Schramm,[159] M. Schreyer,[175] C. Schroeder,[82] N. Schuh,[82] M. J. Schultens,[21] H.-C. Schultz-Coulon,[58a] H. Schulz,[16] M. Schumacher,[48] B. A. Schumm,[138] Ph. Schune,[137] C. Schwanenberger,[83] A. Schwartzman,[144] Ph. Schwegler,[100] Ph. Schwemling,[137] R. Schwienhorst,[89] J. Schwindling,[137] T. Schwindt,[21] M. Schwoerer,[5] F. G. Sciacca,[17] E. Scifo,[116] G. Sciolla,[23] W. G. Scott,[130] F. Scuri,[123a,123b] F. Scutti,[21] J. Searcy,[88] G. Sedov,[42] E. Sedykh,[122] S. C. Seidel,[104] A. Seiden,[138] F. Seifert,[127] J. M. Seixas,[24a] G. Sekhniaidze,[103a] S. J. Sekula,[40] K. E. Selbach,[46] D. M. Seliverstov,[122,a] G. Sellers,[73] N. Semprini-Cesari,[20a,20b] C. Serfon,[30] L. Serin,[116] L. Serkin,[54] T. Serre,[84] R. Seuster,[160a] H. Severini,[112] F. Sforza,[100] A. Sfyrla,[30] E. Shabalina,[54] M. Shamim,[115] L. Y. Shan,[33a] R. Shang,[166] J. T. Shank,[22] Q. T. Shao,[87] M. Shapiro,[15] P. B. Shatalov,[96] K. Shaw,[165a,165b] P. Sherwood,[77] L. Shi,[152,ff] S. Shimizu,[66] C. O. Shimmin,[164] M. Shimojima,[101] M. Shiyakova,[64] A. Shmeleva,[95] M. J. Shochet,[31] D. Short,[119] S. Shrestha,[63] E. Shulga,[97] M. A. Shupe,[7] S. Shushkevich,[42] P. Sicho,[126] O. Sidiropoulou,[155] D. Sidorov,[113] A. Sidoti,[133a] F. Siegert,[44] Dj. Sijacki,[13a] J. Silva,[125a,125d] Y. Silver,[154] D. Silverstein,[144] S. B. Silverstein,[147a] V. Simak,[127] O. Simard,[5] Lj. Simic,[13a] S. Simion,[116] E. Simioni,[82] B. Simmons,[77] R. Simoniello,[90a,90b] M. Simonyan,[36] P. Sinervo,[159] N. B. Sinev,[115] V. Sipica,[142] G. Siragusa,[175] A. Sircar,[78] A. N. Sisakyan,[64,a] S. Yu. Sivoklokov,[98] J. Sjölin,[147a,147b] T. B. Sjursen,[14] H. P. Skottowe,[57] K. Yu. Skovpen,[108] P. Skubic,[112] M. Slater,[18] T. Slavicek,[127] K. Sliwa,[162] V. Smakhtin,[173] B. H. Smart,[46] L. Smestad,[14] S. Yu. Smirnov,[97] Y. Smirnov,[97] L. N. Smirnova,[98,gg] O. Smirnova,[80] K. M. Smith,[53] M. Smizanska,[71] K. Smolek,[127] A. A. Snesarev,[95] G. Snidero,[75] S. Snyder,[25] R. Sobie,[170,j] F. Socher,[44] A. Soffer,[154] D. A. Soh,[152,ff] C. A. Solans,[30] M. Solar,[127] J. Solc,[127] E. Yu. Soldatov,[97] U. Soldevila,[168] E. Solfaroli Camillocci,[133a,133b] A. A. Solodkov,[129] A. Soloshenko,[64] O. V. Solovyanov,[129] V. Solovyev,[122] P. Sommer,[48] H. Y. Song,[33b] N. Soni,[1] A. Sood,[15] A. Sopczak,[127] V. Sopko,[127] B. Sopko,[127] V. Sorin,[12] M. Sosebee,[8] R. Soualah,[165a,165c] P. Soueid,[94] A. M. Soukharev,[108] D. South,[42] S. Spagnolo,[72a,72b] F. Spanò,[76] W. R. Spearman,[57] R. Spighi,[20a] G. Spigo,[30] M. Spousta,[128] T. Spreitzer,[159] B. Spurlock,[8] R. D. St. Denis,[53,a] S. Staerz,[44] J. Stahlman,[121] R. Stamen,[58a] E. Stanecka,[39] R. W. Stanek,[6] C. Stanescu,[135a] M. Stanescu-Bellu,[42] M. M. Stanitzki,[42] S. Stapnes,[118] E. A. Starchenko,[129] J. Stark,[55] P. Staroba,[126] P. Starovoitov,[42] R. Staszewski,[39] P. Stavina,[145a,a] P. Steinberg,[25] B. Stelzer,[143] H. J. Stelzer,[30] O. Stelzer-Chilton,[160a] H. Stenzel,[52] S. Stern,[100] G. A. Stewart,[53] J. A. Stillings,[21] M. C. Stockton,[86] M. Stoebe,[86] G. Stoicea,[26a] P. Stolte,[54] S. Stonjek,[100] A. R. Stradling,[8] A. Straessner,[44] M. E. Stramaglia,[17] J. Strandberg,[148] S. Strandberg,[147a,147b] A. Strandlie,[118] E. Strauss,[144] M. Strauss,[112] P. Strizenec,[145b] R. Ströhmer,[175] D. M. Strom,[115] R. Stroynowski,[40] S. A. Stucci,[17] B. Stugu,[14] N. A. Styles,[42] D. Su,[144] J. Su,[124] HS. Subramania,[3] R. Subramaniam,[78] A. Succurro,[12] Y. Sugaya,[117] C. Suhr,[107] M. Suk,[127] V. V. Sulin,[95] S. Sultansoy,[4c] T. Sumida,[67] X. Sun,[33a] J. E. Sundermann,[48] K. Suruliz,[140] G. Susinno,[37a,37b] M. R. Sutton,[150] Y. Suzuki,[65] M. Svatos,[126] S. Swedish,[169] M. Swiatlowski,[144] I. Sykora,[145a] T. Sykora,[128] D. Ta,[89] K. Tackmann,[42] J. Taenzer,[159] A. Taffard,[164] R. Tafirout,[160a] N. Taiblum,[154] Y. Takahashi,[102] H. Takai,[25] R. Takashima,[68] H. Takeda,[66] T. Takeshita,[141] Y. Takubo,[65] M. Talby,[84] A. A. Talyshev,[108,s] J. Y. C. Tam,[175] K. G. Tan,[87] J. Tanaka,[156] R. Tanaka,[116] S. Tanaka,[132] S. Tanaka,[65] A. J. Tanasijczuk,[143] K. Tani,[66] N. Tannoury,[21] S. Tapprogge,[82] S. Tarem,[153] F. Tarrade,[29] G. F. Tartarelli,[90a] P. Tas,[128] M. Tasevsky,[126] T. Tashiro,[67] E. Tassi,[37a,37b] A. Tavares Delgado,[125a,125b] Y. Tayalati,[136d] F. E. Taylor,[93] G. N. Taylor,[87] W. Taylor,[160b] F. A. Teischinger,[30] M. Teixeira Dias Castanheira,[75] P. Teixeira-Dias,[76] K. K. Temming,[48] H. Ten Kate,[30] P. K. Teng,[152] J. J. Teoh,[117] S. Terada,[65] K. Terashi,[156] J. Terron,[81] S. Terzo,[100] M. Testa,[47] R. J. Teuscher,[159,j] J. Therhaag,[21] T. Theveneaux-Pelzer,[34] J. P. Thomas,[18] J. Thomas-Wilsker,[76] E. N. Thompson,[35] P. D. Thompson,[18] P. D. Thompson,[159] A. S. Thompson,[53] L. A. Thomsen,[36] E. Thomson,[121] M. Thomson,[28] W. M. Thong,[87] R. P. Thun,[88,a] F. Tian,[35] M. J. Tibbetts,[15] V. O. Tikhomirov,[95,hh] Yu. A. Tikhonov,[108,s] S. Timoshenko,[97] E. Tiouchichine,[84] P. Tipton,[177] S. Tisserant,[84] T. Todorov,[5] S. Todorova-Nova,[128] B. Toggerson,[7] J. Tojo,[69] S. Tokár,[145a] K. Tokushuku,[65] K. Tollefson,[89] L. Tomlinson,[83] M. Tomoto,[102] L. Tompkins,[31] K. Toms,[104] N. D. Topilin,[64] E. Torrence,[115] H. Torres,[143] E. Torró Pastor,[168] J. Toth,[84,ii] F. Touchard,[84] D. R. Tovey,[140] H. L. Tran,[116] T. Trefzger,[175] L. Tremblet,[30] A. Tricoli,[30] I. M. Trigger,[160a] S. Trincaz-Duvoid,[79] M. F. Tripiana,[70] N. Triplett,[25] W. Trischuk,[159] B. Trocmé,[55] C. Troncon,[90a] M. Trottier-McDonald,[143] M. Trovatelli,[135a,135b] P. True,[89]

M. Trzebinski,[39] A. Trzupek,[39] C. Tsarouchas,[30] J. C-L. Tseng,[119] P. V. Tsiareshka,[91] D. Tsionou,[137] G. Tsipolitis,[10] N. Tsirintanis,[9] S. Tsiskaridze,[12] V. Tsiskaridze,[48] E. G. Tskhadadze,[51a] I. I. Tsukerman,[96] V. Tsulaia,[15] S. Tsuno,[65] D. Tsybychev,[149] A. Tudorache,[26a] V. Tudorache,[26a] A. N. Tuna,[121] S. A. Tupputi,[20a,20b] S. Turchikhin,[98,gg] D. Turecek,[127] I. Turk Cakir,[4d] R. Turra,[90a,90b] P. M. Tuts,[35] A. Tykhonov,[74] M. Tylmad,[147a,147b] M. Tyndel,[130] K. Uchida,[21] I. Ueda,[156] R. Ueno,[29] M. Ughetto,[84] M. Ugland,[14] M. Uhlenbrock,[21] F. Ukegawa,[161] G. Unal,[30] A. Undrus,[25] G. Unel,[164] F. C. Ungaro,[48] Y. Unno,[65] D. Urbaniec,[35] P. Urquijo,[21] G. Usai,[8] A. Usanova,[61] L. Vacavant,[84] V. Vacek,[127] B. Vachon,[86] N. Valencic,[106] S. Valentinetti,[20a,20b] A. Valero,[168] L. Valery,[34] S. Valkar,[128] E. Valladolid Gallego,[168] S. Vallecorsa,[49] J. A. Valls Ferrer,[168] P. C. Van Der Deijl,[106] R. van der Geer,[106] H. van der Graaf,[106] R. Van Der Leeuw,[106] D. van der Ster,[30] N. van Eldik,[30] P. van Gemmeren,[6] J. Van Nieuwkoop,[143] I. van Vulpen,[106] M. C. van Woerden,[30] M. Vanadia,[133a,133b] W. Vandelli,[30] R. Vanguri,[121] A. Vaniachine,[6] P. Vankov,[42] F. Vannucci,[79] G. Vardanyan,[178] R. Vari,[133a] E. W. Varnes,[7] T. Varol,[85] D. Varouchas,[79] A. Vartapetian,[8] K. E. Varvell,[151] F. Vazeille,[34] T. Vazquez Schroeder,[54] J. Veatch,[7] F. Veloso,[125a,125c] S. Veneziano,[133a] A. Ventura,[72a,72b] D. Ventura,[85] M. Venturi,[170] N. Venturi,[159] A. Venturini,[23] V. Vercesi,[120a] M. Verducci,[139] W. Verkerke,[106] J. C. Vermeulen,[106] A. Vest,[44] M. C. Vetterli,[143,f] O. Viazlo,[80] I. Vichou,[166] T. Vickey,[146c,jj] O. E. Vickey Boeriu,[146c] G. H. A. Viehhauser,[119] S. Viel,[169] R. Vigne,[30] M. Villa,[20a,20b] M. Villaplana Perez,[90a,90b] E. Vilucchi,[47] M. G. Vincter,[29] V. B. Vinogradov,[64] J. Virzi,[15] I. Vivarelli,[150] F. Vives Vaque,[3] S. Vlachos,[10] D. Vladoiu,[99] M. Vlasak,[127] A. Vogel,[21] M. Vogel,[32a] P. Vokac,[127] G. Volpi,[123a,123b] M. Volpi,[87] H. von der Schmitt,[100] H. von Radziewski,[48] E. von Toerne,[21] V. Vorobel,[128] K. Vorobev,[97] M. Vos,[168] R. Voss,[30] J. H. Vossebeld,[73] N. Vranjes,[137] M. Vranjes Milosavljevic,[106] V. Vrba,[126] M. Vreeswijk,[106] T. Vu Anh,[48] R. Vuillermet,[30] I. Vukotic,[31] Z. Vykydal,[127] W. Wagner,[176] P. Wagner,[21] H. Wahlberg,[70] S. Wahrmund,[44] J. Wakabayashi,[102] J. Walder,[71] R. Walker,[99] W. Walkowiak,[142] R. Wall,[177] P. Waller,[73] B. Walsh,[177] C. Wang,[152,kk] C. Wang,[45] F. Wang,[174] H. Wang,[15] H. Wang,[40] J. Wang,[42] J. Wang,[33a] K. Wang,[86] R. Wang,[104] S. M. Wang,[152] T. Wang,[21] X. Wang,[177] C. Wanotayaroj,[115] A. Warburton,[86] C. P. Ward,[28] D. R. Wardrope,[77] M. Warsinsky,[48] A. Washbrook,[46] C. Wasicki,[42] I. Watanabe,[66] P. M. Watkins,[18] A. T. Watson,[18] I. J. Watson,[151] M. F. Watson,[18] G. Watts,[139] S. Watts,[83] B. M. Waugh,[77] S. Webb,[83] M. S. Weber,[17] S. W. Weber,[175] J. S. Webster,[31] A. R. Weidberg,[119] P. Weigell,[100] B. Weinert,[60] J. Weingarten,[54] C. Weiser,[48] H. Weits,[106] P. S. Wells,[30] T. Wenaus,[25] D. Wendland,[16] Z. Weng,[152,ff] T. Wengler,[30] S. Wenig,[30] N. Wermes,[21] M. Werner,[48] P. Werner,[30] M. Wessels,[58a] J. Wetter,[162] K. Whalen,[29] A. White,[8] M. J. White,[1] R. White,[32b] S. White,[123a,123b] D. Whiteson,[164] D. Wicke,[176] F. J. Wickens,[130] W. Wiedenmann,[174] M. Wielers,[130] P. Wienemann,[21] C. Wiglesworth,[36] L. A. M. Wiik-Fuchs,[21] P. A. Wijeratne,[77] A. Wildauer,[100] M. A. Wildt,[42,ll] H. G. Wilkens,[30] J. Z. Will,[99] H. H. Williams,[121] S. Williams,[28] C. Willis,[89] S. Willocq,[85] J. A. Wilson,[18] A. Wilson,[88] I. Wingerter-Seez,[5] F. Winklmeier,[115] B. T. Winter,[21] M. Wittgen,[144] T. Wittig,[43] J. Wittkowski,[99] S. J. Wollstadt,[82] M. W. Wolter,[39] H. Wolters,[125a,125c] B. K. Wosiek,[39] J. Wotschack,[30] M. J. Woudstra,[83] K. W. Wozniak,[39] M. Wright,[53] M. Wu,[55] S. L. Wu,[174] X. Wu,[49] Y. Wu,[88] E. Wulf,[35] T. R. Wyatt,[83] B. M. Wynne,[46] S. Xella,[36] M. Xiao,[137] D. Xu,[33a] L. Xu,[33b,mm] B. Yabsley,[151] S. Yacoob,[146b,nn] M. Yamada,[65] H. Yamaguchi,[156] Y. Yamaguchi,[156] A. Yamamoto,[65] K. Yamamoto,[63] S. Yamamoto,[156] T. Yamamura,[156] T. Yamanaka,[156] K. Yamauchi,[102] Y. Yamazaki,[66] Z. Yan,[22] H. Yang,[33e] H. Yang,[174] U. K. Yang,[83] Y. Yang,[110] S. Yanush,[92] L. Yao,[33a] W-M. Yao,[15] Y. Yasu,[65] E. Yatsenko,[42] K. H. Yau Wong,[21] J. Ye,[40] S. Ye,[25] I. Yeletskikh,[64] A. L. Yen,[57] E. Yildirim,[42] M. Yilmaz,[4b] R. Yoosoofmiya,[124] K. Yorita,[172] R. Yoshida,[6] K. Yoshihara,[156] C. Young,[144] C. J. S. Young,[30] S. Youssef,[22] D. R. Yu,[15] J. Yu,[8] J. M. Yu,[88] J. Yu,[113] L. Yuan,[66] A. Yurkewicz,[107] B. Zabinski,[39] R. Zaidan,[62] A. M. Zaitsev,[129,z] A. Zaman,[149] S. Zambito,[23] L. Zanello,[133a,133b] D. Zanzi,[100] C. Zeitnitz,[176] M. Zeman,[127] A. Zemla,[38a] K. Zengel,[23] O. Zenin,[129] T. Ženiš,[145a] D. Zerwas,[116] G. Zevi della Porta,[57] D. Zhang,[88] F. Zhang,[174] H. Zhang,[89] J. Zhang,[6] L. Zhang,[152] X. Zhang,[33d] Z. Zhang,[116] Z. Zhao,[33b] A. Zhemchugov,[64] J. Zhong,[119] B. Zhou,[88] L. Zhou,[35] N. Zhou,[164] C. G. Zhu,[33d] H. Zhu,[33a] J. Zhu,[88] Y. Zhu,[33b] X. Zhuang,[33a] A. Zibell,[175] D. Zieminska,[60] N. I. Zimine,[64] C. Zimmermann,[82] R. Zimmermann,[21] S. Zimmermann,[21] S. Zimmermann,[48] Z. Zinonos,[54] M. Zinser,[82] M. Ziolkowski,[142] G. Zobernig,[174] A. Zoccoli,[20a,20b] M. zur Nedden,[16] G. Zurzolo,[103a,103b] V. Zutshi[107] and L. Zwalinski[30]

(ATLAS Collaboration)

[1]*Department of Physics, University of Adelaide, Adelaide, Australia*
[2]*Physics Department, SUNY Albany, Albany, New York, USA*
[3]*Department of Physics, University of Alberta, Edmonton Albeta, Canada*
[4a]*Department of Physics, Ankara University, Ankara, Turkey*

[4b]*Department of Physics, Gazi University, Ankara, Turkey*
[4c]*Division of Physics, TOBB University of Economics and Technology, Ankara, Turkey*
[4d]*Turkish Atomic Energy Authority, Ankara, Turkey*
[5]*LAPP, CNRS/IN2P3 and Université de Savoie, Annecy-le-Vieux, France*
[6]*High Energy Physics Division, Argonne National Laboratory, Argonne, Illinois, USA*
[7]*Department of Physics, University of Arizona, Tucson, Arizona, USA*
[8]*Department of Physics, The University of Texas at Arlington, Arlington, Texas, USA*
[9]*Physics Department, University of Athens, Athens, Greece*
[10]*Physics Department, National Technical University of Athens, Zografou, Greece*
[11]*Institute of Physics, Azerbaijan Academy of Sciences, Baku, Azerbaijan*
[12]*Institut de Física d'Altes Energies and Departament de Física de la Universitat Autònoma de Barcelona, Barcelona, Spain*
[13a]*Institute of Physics, University of Belgrade, Belgrade, Serbia*
[13b]*Vinca Institute of Nuclear Sciences, University of Belgrade, Belgrade, Serbia*
[14]*Department for Physics and Technology, University of Bergen, Bergen, Norway*
[15]*Physics Division, Lawrence Berkeley National Laboratory and University of California, Berkeley, California, USA*
[16]*Department of Physics, Humboldt University, Berlin, Germany*
[17]*Albert Einstein Center for Fundamental Physics and Laboratory for High Energy Physics, University of Bern, Bern, Switzerland*
[18]*School of Physics and Astronomy, University of Birmingham, Birmingham, United Kingdom*
[19a]*Department of Physics, Bogazici University, Istanbul, Turkey*
[19b]*Department of Physics, Dogus University, Istanbul, Turkey*
[19c]*Department of Physics Engineering, Gaziantep University, Gaziantep, Turkey*
[20a]*INFN Sezione di Bologna, Bologna, Italy*
[20b]*Dipartimento di Fisica e Astronomia, Università di Bologna, Bologna, Italy*
[21]*Physikalisches Institut, University of Bonn, Bonn, Germany*
[22]*Department of Physics, Boston University, Boston, Massachusetts, USA*
[23]*Department of Physics, Brandeis University, Waltham, Massachusetts, USA*
[24a]*Universidade Federal do Rio De Janeiro COPPE/EE/IF, Rio de Janeiro, Brazil*
[24b]*Federal University of Juiz de Fora (UFJF), Juiz de Fora, Brazil*
[24c]*Federal University of Sao Joao del Rei (UFSJ), Sao Joao del Rei, Brazil*
[24d]*Instituto de Fisica, Universidade de Sao Paulo, Sao Paulo, Brazil*
[25]*Physics Department, Brookhaven National Laboratory, Upton, New York, USA*
[26a]*National Institute of Physics and Nuclear Engineering, Bucharest, Romania*
[26b]*National Institute for Research and Development of Isotopic and Molecular Technologies, Physics Department, Cluj Napoca, Romania*
[26c]*University Politehnica Bucharest, Bucharest, Romania*
[26d]*West University in Timisoara, Timisoara, Romania*
[27]*Departamento de Física, Universidad de Buenos Aires, Buenos Aires, Argentina*
[28]*Cavendish Laboratory, University of Cambridge, Cambridge, United Kingdom*
[29]*Department of Physics, Carleton University, Ottawa, Ontario, Canada*
[30]*CERN, Geneva, Switzerland*
[31]*Enrico Fermi Institute, University of Chicago, Chicago, Illinois, USA*
[32a]*Departamento de Física, Pontificia Universidad Católica de Chile, Santiago, Chile*
[32b]*Departamento de Física, Universidad Técnica Federico Santa María, Valparaíso, Chile*
[33a]*Institute of High Energy Physics, Chinese Academy of Sciences, Beijing, People's Republic of China*
[33b]*Department of Modern Physics, University of Science and Technology of China, Anhui, People's Republic of China*
[33c]*Department of Physics, Nanjing University, Jiangsu, People's Republic of China*
[33d]*School of Physics, Shandong University, Shandong, People's Republic of China*
[33e]*Physics Department, Shanghai Jiao Tong University, Shanghai, People's Republic of China*
[34]*Laboratoire de Physique Corpusculaire, Clermont Université and Université Blaise Pascal and CNRS/IN2P3, Clermont-Ferrand, France*
[35]*Nevis Laboratory, Columbia University, Irvington, New York, USA*
[36]*Niels Bohr Institute, University of Copenhagen, Kobenhavn, Denmark*
[37a]*INFN Gruppo Collegato di Cosenza, Laboratori Nazionali di Frascati, Italy*
[37b]*Dipartimento di Fisica, Università della Calabria, Rende, Italy*
[38a]*AGH University of Science and Technology, Faculty of Physics and Applied Computer Science, Krakow, Poland*

[38b]Marian Smoluchowski Institute of Physics, Jagiellonian University, Krakow, Poland
[39]The Henryk Niewodniczanski Institute of Nuclear Physics, Polish Academy of Sciences, Krakow, Poland
[40]Physics Department, Southern Methodist University, Dallas, Texas, USA
[41]Physics Department, University of Texas at Dallas, Richardson, Texas, USA
[42]DESY, Hamburg and Zeuthen, Germany
[43]Institut für Experimentelle Physik IV, Technische Universität Dortmund, Dortmund, Germany
[44]Institut für Kern- und Teilchenphysik, Technische Universität Dresden, Dresden, Germany
[45]Department of Physics, Duke University, Durham, North Carolina, USA
[46]SUPA - School of Physics and Astronomy, University of Edinburgh, Edinburgh, United Kingdom
[47]INFN Laboratori Nazionali di Frascati, Frascati, Italy
[48]Fakultät für Mathematik und Physik, Albert-Ludwigs-Universität, Freiburg, Germany
[49]Section de Physique, Université de Genève, Geneva, Switzerland
[50a]INFN Sezione di Genova, Genova, Italy
[50b]Dipartimento di Fisica, Università di Genova, Genova, Italy
[51a]E. Andronikashvili Institute of Physics, Iv. Javakhishvili Tbilisi State University, Tbilisi, Georgia
[51b]High Energy Physics Institute, Tbilisi State University, Tbilisi, Georgia
[52]II Physikalisches Institut, Justus-Liebig-Universität Giessen, Giessen, Germany
[53]SUPA - School of Physics and Astronomy, University of Glasgow, Glasgow, United Kingdom
[54]II Physikalisches Institut, Georg-August-Universität, Göttingen, Germany
[55]Laboratoire de Physique Subatomique et de Cosmologie, Université Grenoble-Alpes, CNRS/IN2P3, Grenoble, France
[56]Department of Physics, Hampton University, Hampton, Virginia, USA
[57]Laboratory for Particle Physics and Cosmology, Harvard University, Cambridge, Massachusetts, USA
[58a]Kirchhoff-Institut für Physik, Ruprecht-Karls-Universität Heidelberg, Heidelberg, Germany
[58b]Physikalisches Institut, Ruprecht-Karls-Universität Heidelberg, Heidelberg, Germany
[58c]ZITI Institut für technische Informatik, Ruprecht-Karls-Universität Heidelberg, Mannheim, Germany
[59]Faculty of Applied Information Science, Hiroshima Institute of Technology, Hiroshima, Japan
[60]Department of Physics, Indiana University, Bloomington, Indiana, USA
[61]Institut für Astro- und Teilchenphysik, Leopold-Franzens-Universität, Innsbruck, Austria
[62]University of Iowa, Iowa City, Iowa, USA
[63]Department of Physics and Astronomy, Iowa State University, Ames, Iowa, USA
[64]Joint Institute for Nuclear Research, JINR Dubna, Dubna, Russia
[65]KEK, High Energy Accelerator Research Organization, Tsukuba, Japan
[66]Graduate School of Science, Kobe University, Kobe, Japan
[67]Faculty of Science, Kyoto University, Kyoto, Japan
[68]Kyoto University of Education, Kyoto, Japan
[69]Department of Physics, Kyushu University, Fukuoka, Japan
[70]Instituto de Física La Plata, Universidad Nacional de La Plata and CONICET, La Plata, Argentina
[71]Physics Department, Lancaster University, Lancaster, United Kingdom
[72a]INFN Sezione di Lecce, Lecce, Italy
[72b]Dipartimento di Matematica e Fisica, Università del Salento, Lecce, Italy
[73]Oliver Lodge Laboratory, University of Liverpool, Liverpool, United Kingdom
[74]Department of Physics, Jožef Stefan Institute and University of Ljubljana, Ljubljana, Slovenia
[75]School of Physics and Astronomy, Queen Mary University of London, London, United Kingdom
[76]Department of Physics, Royal Holloway University of London, Surrey, United Kingdom
[77]Department of Physics and Astronomy, University College London, London, United Kingdom
[78]Louisiana Tech University, Ruston, Louisiana, USA
[79]Laboratoire de Physique Nucléaire et de Hautes Energies, UPMC and Université Paris-Diderot and CNRS/IN2P3, Paris, France
[80]Fysiska institutionen, Lunds universitet, Lund, Sweden
[81]Departamento de Fisica Teorica C-15, Universidad Autonoma de Madrid, Madrid, Spain
[82]Institut für Physik, Universität Mainz, Mainz, Germany
[83]School of Physics and Astronomy, University of Manchester, Manchester, United Kingdom
[84]CPPM, Aix-Marseille Université and CNRS/IN2P3, Marseille, France
[85]Department of Physics, University of Massachusetts, Amherst, Massachusetts, USA
[86]Department of Physics, McGill University, Montreal, Quebec, Canada
[87]School of Physics, University of Melbourne, Victoria, Australia
[88]Department of Physics, The University of Michigan, Ann Arbor, Michigan, USA
[89]Department of Physics and Astronomy, Michigan State University, East Lansing, Michigan, USA
[90a]INFN Sezione di Milano, Milano, Italy

[90b]*Dipartimento di Fisica, Università di Milano, Milano, Italy*
[91]*B. I. Stepanov Institute of Physics, National Academy of Sciences of Belarus, Minsk, Republic of Belarus*
[92]*National Scientific and Educational Centre for Particle and High Energy Physics, Minsk, Belarus*
[93]*Department of Physics, Massachusetts Institute of Technology, Cambridge, Massachusetts, USA*
[94]*Group of Particle Physics, University of Montreal, Montreal, Quebec, Canada*
[95]*P. N. Lebedev Institute of Physics, Academy of Sciences, Moscow, Russia*
[96]*Institute for Theoretical and Experimental Physics (ITEP), Moscow, Russia*
[97]*Moscow Engineering and Physics Institute (MEPhI), Moscow, Russia*
[98]*D. V. Skobeltsyn Institute of Nuclear Physics, M. V. Lomonosov Moscow State University, Moscow, Russia*
[99]*Fakultät für Physik, Ludwig-Maximilians-Universität München, München, Germany*
[100]*Max-Planck-Institut für Physik (Werner-Heisenberg-Institut), München, Germany*
[101]*Nagasaki Institute of Applied Science, Nagasaki, Japan*
[102]*Graduate School of Science and Kobayashi-Maskawa Institute, Nagoya University, Nagoya, Japan*
[103a]*INFN Sezione di Napoli, Napoli, Italy*
[103b]*Dipartimento di Fisica, Università di Napoli, Napoli, Italy*
[104]*Department of Physics and Astronomy, University of New Mexico, Albuquerque, New Mexico, USA*
[105]*Institute for Mathematics, Astrophysics and Particle Physics, Radboud University Nijmegen/Nikhef, Nijmegen, Netherlands*
[106]*Nikhef National Institute for Subatomic Physics and University of Amsterdam, Amsterdam, Netherlands*
[107]*Department of Physics, Northern Illinois University, DeKalb, Illinois, USA*
[108]*Budker Institute of Nuclear Physics, SB RAS, Novosibirsk, Russia*
[109]*Department of Physics, New York University, New York, New York, USA*
[110]*Ohio State University, Columbus, Ohio, USA*
[111]*Faculty of Science, Okayama University, Okayama, Japan*
[112]*Homer L. Dodge Department of Physics and Astronomy, University of Oklahoma, Norman, Oklahoma, USA*
[113]*Department of Physics, Oklahoma State University, Stillwater, Oklahoma, USA*
[114]*Palacký University, RCPTM, Olomouc, Czech Republic*
[115]*Center for High Energy Physics, University of Oregon, Eugene, Oregon, USA*
[116]*LAL, Université Paris-Sud and CNRS/IN2P3, Orsay, France*
[117]*Graduate School of Science, Osaka University, Osaka, Japan*
[118]*Department of Physics, University of Oslo, Oslo, Norway*
[119]*Department of Physics, Oxford University, Oxford, United Kingdom*
[120a]*INFN Sezione di Pavia, Pavia, Italy*
[120b]*Dipartimento di Fisica, Università di Pavia, Pavia, Italy*
[121]*Department of Physics, University of Pennsylvania, Philadelphia, Pennsylvania, USA*
[122]*Petersburg Nuclear Physics Institute, Gatchina, Russia*
[123a]*INFN Sezione di Pisa, Pisa, Italy*
[123b]*Dipartimento di Fisica E. Fermi, Università di Pisa, Pisa, Italy*
[124]*Department of Physics and Astronomy, University of Pittsburgh, Pittsburgh, Pennsylvania, USA*
[125a]*Laboratorio de Instrumentacao e Fisica Experimental de Particulas - LIP, Lisboa, Portugal*
[125b]*Faculdade de Ciências, Universidade de Lisboa, Lisboa, Portugal*
[125c]*Department of Physics, University of Coimbra, Coimbra, Portugal*
[125d]*Centro de Física Nuclear da Universidade de Lisboa, Lisboa, Portugal*
[125e]*Departamento de Fisica, Universidade do Minho, Braga, Portugal*
[125f]*Departamento de Fisica Teorica y del Cosmos and CAFPE, Universidad de Granada, Granada, Spain*
[125g]*Dep Fisica and CEFITEC of Faculdade de Ciencias e Tecnologia, Universidade Nova de Lisboa, Caparica, Portugal*
[126]*Institute of Physics, Academy of Sciences of the Czech Republic, Praha, Czech Republic*
[127]*Czech Technical University in Prague, Praha, Czech Republic*
[128]*Faculty of Mathematics and Physics, Charles University in Prague, Praha, Czech Republic*
[129]*State Research Center Institute for High Energy Physics, Protvino, Russia*
[130]*Particle Physics Department, Rutherford Appleton Laboratory, Didcot, United Kingdom*
[131]*Physics Department, University of Regina, Regina, Saskatchewan, Canada*
[132]*Ritsumeikan University, Kusatsu, Shiga, Japan*
[133a]*INFN Sezione di Roma, Roma, Italy*
[133b]*Dipartimento di Fisica, Sapienza Università di Roma, Roma, Italy*

[134a]*INFN Sezione di Roma Tor Vergata, Roma, Italy*
[134b]*Dipartimento di Fisica, Università di Roma Tor Vergata, Roma, Italy*
[135a]*INFN Sezione di Roma Tre, Roma, Italy*
[135b]*Dipartimento di Matematica e Fisica, Università Roma Tre, Roma, Italy*
[136a]*Faculté des Sciences Ain Chock, Réseau Universitaire de Physique des Hautes Energies - Université Hassan II, Casablanca, Morocco, Morocco*
[136b]*Centre National de l'Energie des Sciences Techniques Nucleaires, Rabat, Morocco*
[136c]*Faculté des Sciences Semlalia, Université Cadi Ayyad, LPHEA-Marrakech, Morocco*
[136d]*Faculté des Sciences, Université Mohamed Premier and LPTPM, Oujda, Morocco*
[136e]*Faculté des sciences, Université Mohammed V-Agdal, Rabat, Morocco*
[137]*DSM/IRFU (Institut de Recherches sur les Lois Fondamentales de l'Univers), CEA Saclay (Commissariat à l'Energie Atomique et aux Energies Alternatives), Gif-sur-Yvette, France*
[138]*Santa Cruz Institute for Particle Physics, University of California Santa Cruz, Santa Cruz, California, USA*
[139]*Department of Physics, University of Washington, Seattle, Washington, USA*
[140]*Department of Physics and Astronomy, University of Sheffield, Sheffield, United Kingdom*
[141]*Department of Physics, Shinshu University, Nagano, Japan*
[142]*Fachbereich Physik, Universität Siegen, Siegen, Germany*
[143]*Department of Physics, Simon Fraser University, Burnaby, British Columbia, Canada*
[144]*SLAC National Accelerator Laboratory, Stanford, California, USA*
[145a]*Faculty of Mathematics, Physics & Informatics, Comenius University, Bratislava, Slovak Republic*
[145b]*Department of Subnuclear Physics, Institute of Experimental Physics of the Slovak Academy of Sciences, Kosice, Slovak Republic*
[146a]*Department of Physics, University of Cape Town, Cape Town, South Africa*
[146b]*Department of Physics, University of Johannesburg, Johannesburg, South Africa*
[146c]*School of Physics, University of the Witwatersrand, Johannesburg, South Africa*
[147a]*Department of Physics, Stockholm University, Stockholm, Sweden*
[147b]*The Oskar Klein Centre, Stockholm, Sweden*
[148]*Physics Department, Royal Institute of Technology, Stockholm, Sweden*
[149]*Departments of Physics & Astronomy and Chemistry, Stony Brook University, Stony Brook, New York, USA*
[150]*Department of Physics and Astronomy, University of Sussex, Brighton, United Kingdom*
[151]*School of Physics, University of Sydney, Sydney, Australia*
[152]*Institute of Physics, Academia Sinica, Taipei, Taiwan*
[153]*Department of Physics, Technion: Israel Institute of Technology, Haifa, Israel*
[154]*Raymond and Beverly Sackler School of Physics and Astronomy, Tel Aviv University, Tel Aviv, Israel*
[155]*Department of Physics, Aristotle University of Thessaloniki, Thessaloniki, Greece*
[156]*International Center for Elementary Particle Physics and Department of Physics, The University of Tokyo, Tokyo, Japan*
[157]*Graduate School of Science and Technology, Tokyo Metropolitan University, Tokyo, Japan*
[158]*Department of Physics, Tokyo Institute of Technology, Tokyo, Japan*
[159]*Department of Physics, University of Toronto, Toronto, Ontario, Canada*
[160a]*TRIUMF, Vancouver, British Columbia, Canada*
[160b]*Department of Physics and Astronomy, York University, Toronto, Ontario, Canada*
[161]*Faculty of Pure and Applied Sciences, University of Tsukuba, Tsukuba, Japan*
[162]*Department of Physics and Astronomy, Tufts University, Medford, Massachusetts, USA*
[163]*Centro de Investigaciones, Universidad Antonio Narino, Bogota, Colombia*
[164]*Department of Physics and Astronomy, University of California Irvine, Irvine, California, USA*
[165a]*INFN Gruppo Collegato di Udine, Sezione di Trieste, Udine, Italy*
[165b]*ICTP, Trieste, Italy*
[165c]*Dipartimento di Chimica, Fisica e Ambiente, Università di Udine, Udine, Italy*
[166]*Department of Physics, University of Illinois, Urbana, Illinois, USA*
[167]*Department of Physics and Astronomy, University of Uppsala, Uppsala, Sweden*
[168]*Instituto de Física Corpuscular (IFIC) and Departamento de Física Atómica, Molecular y Nuclear and Departamento de Ingeniería Electrónica and Instituto de Microelectrónica de Barcelona (IMB-CNM), University of Valencia and CSIC, Valencia, Spain*
[169]*Department of Physics, University of British Columbia, Vancouver, British Columbia, Canada*
[170]*Department of Physics and Astronomy, University of Victoria, Victoria, British Columbia, Canada*
[171]*Department of Physics, University of Warwick, Coventry, United Kingdom*
[172]*Waseda University, Tokyo, Japan*

[173]*Department of Particle Physics, The Weizmann Institute of Science, Rehovot, Israel*
[174]*Department of Physics, University of Wisconsin, Madison, Wisconsin, USA*
[175]*Fakultät für Physik und Astronomie, Julius-Maximilians-Universität, Würzburg, Germany*
[176]*Fachbereich C Physik, Bergische Universität Wuppertal, Wuppertal, Germany*
[177]*Department of Physics, Yale University, New Haven, Connecticut, USA*
[178]*Yerevan Physics Institute, Yerevan, Armenia*
[179]*Centre de Calcul de l'Institut National de Physique Nucléaire et de Physique des Particules (IN2P3), Villeurbanne, France*

[a]Deceased.
[b]Also at Department of Physics, King's College London, London, United Kingdom.
[c]Also at Institute of Physics, Azerbaijan Academy of Sciences, Baku, Azerbaijan.
[d]Also at Department of Physics, University of British Columbia, Vancouver, British Columbia, Canada.
[e]Also at Particle Physics Department, Rutherford Appleton Laboratory, Didcot, United Kingdom.
[f]Also at TRIUMF, Vancouver, British Columbia, Canada.
[g]Also at Department of Physics, California State University, Fresno, California, USA.
[h]Also at CPPM, Aix-Marseille Université and CNRS/IN2P3, Marseille, France.
[i]Also at Università di Napoli Parthenope, Napoli, Italy.
[j]Also at Institute of Particle Physics (IPP), Canada.
[k]Also at Department of Physics, St. Petersburg State Polytechnical University, St. Petersburg, Russia.
[l]Also at Department of Financial and Management Engineering, University of the Aegean, Chios, Greece.
[m]Also at Louisiana Tech University, Ruston, Los Angeles, USA.
[n]Also at Institucio Catalana de Recerca i Estudis Avancats, ICREA, Barcelona, Spain.
[o]Also at Institute of Theoretical Physics, Ilia State University, Tbilisi, Georgia.
[p]Also at CERN, Geneva, Switzerland.
[q]Also at Ochadai Academic Production, Ochanomizu University, Tokyo, Japan.
[r]Also at Manhattan College, New York, New York, USA.
[s]Also at Novosibirsk State University, Novosibirsk, Russia.
[t]Also at Institute of Physics, Academia Sinica, Taipei, Taiwan.
[u]Also at LAL, Université Paris-Sud and CNRS/IN2P3, Orsay, France.
[v]Also at Academia Sinica Grid Computing, Institute of Physics, Academia Sinica, Taipei, Taiwan.
[w]Also at Laboratoire de Physique Nucléaire et de Hautes Energies, UPMC and Université Paris-Diderot and CNRS/IN2P3, Paris, France.
[x]Also at School of Physical Sciences, National Institute of Science Education and Research, Bhubaneswar, India.
[y]Also at Dipartimento di Fisica, Sapienza Università di Roma, Roma, Italy.
[z]Also at Moscow Institute of Physics and Technology State University, Dolgoprudny, Russia.
[aa]Also at Section de Physique, Université de Genève, Geneva, Switzerland.
[bb]Also at Department of Physics, The University of Texas at Austin, Austin, Texas, USA.
[cc]Also at International School for Advanced Studies (SISSA), Trieste, Italy.
[dd]Also at Department of Physics and Astronomy, University of South Carolina, Columbia, South Carolina, USA.
[ee]Associated author at CP3-Origins, University of Southern Denmark, Odense, Denmark.
[ff]Also at School of Physics and Engineering, Sun Yat-sen University, Guangzhou, People's Republic of China.
[ii]Also at Faculty of Physics, M. V. Lomonosov Moscow State University, Moscow, Russia.
[jj]Also at Moscow Engineering and Physics Institute (MEPhI), Moscow, Russia.
[kk]Also at Institute for Particle and Nuclear Physics, Wigner Research Centre for Physics, Budapest, Hungary.
[ll]Also at Department of Physics, Oxford University, Oxford, United Kingdom.
[mm]Also at Department of Physics, Nanjing University, Jiangsu, People's Republic of China.
[nn]Also at Institut für Experimentalphysik, Universität Hamburg, Hamburg, Germany.
[oo]Also at Department of Physics, The University of Michigan, Ann Arbor, Michigan, USA.
[pp]Also at Discipline of Physics, University of KwaZulu-Natal, Durban, South Africa.